Bulletin of the New Zealand Society for Earthquake Engineering, Vol. 49, No. 3, September 2016

NUMERICAL METHODOLOGY FOR DYNAMIC ANALYSIS OF BUILDINGS WITH FRICTION DAMPERS

Subhransu S. Swain[1], Sanjaya K. Patro[2] and Ravi Sinha[3]

(Submitted *February 2015*; Reviewed *July 2015*; Accepted *June 2016*)

ABSTRACT

A number of studies on using friction based energy dissipation system for seismic protection of the building have been published in the recent past. The studies show that numerical approximation of the effectiveness of the friction based energy dissipation system depends on the accurate solution of the relevant nonlinear equations of motion. The available numerical models to idealize the behaviour of friction dampers can be categorized into equivalent linearization method, approximation by rigid-perfectly plastic hysteric model and stick-slide condition model. However, it has been observed that the minimum difference in relative velocity or non-identification of exact time of phase transition from stick to slide condition results in a noticeably high fluctuation of relative velocity in the stick-slide model.

To identify the exact time for phase transition, this paper presents a numerical methodology for dynamic analysis of buildings with friction damper, leading to improved accuracy of solutions of equations of motion. The mathematical formulation and solution procedure of the proposed methodology has been presented in detail in this paper. The results obtained have been validated with examples from published literature. The response of single degree of freedom (SDOF) system with friction device when subjected to nine different ground motions are presented. The selected ground motion encompasses three ground motions each from soft soil, medium soil and hard soil to evaluate the likely response of the structure under the likely range of expected ground motion characteristics. The spectral variation with reference to pretension force has been investigated and presented. The results indicate that for a particular range of pretension force, beyond a particular stiffness ratio, the reduction in spectral response of the damper added system is independent of frequency of the SDOF system, which shows the robustness of friction devices.

INTRODUCTION

The use of friction dampers for seismic protection of buildings has attracted the attention of researchers in the recent past. Friction dampers, which dissipate energy through friction force, have been observed to be used efficiently in structures for reduction of earthquake induced vibrations. In these dampers, a large amount of energy is dissipated in the form of heat during earthquake excitation due to frictional resistance developed between moving solid interfaces, at a predefined load. Friction devices can also be designed to decouple structural fundamental frequencies from dominant frequencies of earthquake ground motion.

Pall et al. [1] developed limited slip bolts (LSB) for the seismic control of precast and cast-in-place concrete walls. The development of friction dampers [1] began by conducting static and dynamic tests on a variety of simple sliding elements having different surface treatments. The goal was not necessarily to obtain maximum energy dissipation, but rather to identify a system that possesses consistent and predictable response. Experimental results by Pall and Marsh [2] have shown that the hysteretic behaviour of the sliding friction joints is reliable and repeatable, and approaches a rectangular hysteretic loop with insignificant degradation over cycles much greater than that encountered in consecutive earthquakes. They also showed that the friction joints should be tuned in order to optimize seismic performance. However, the study considered only one earthquake record and hence the influence of the seismic excitation characteristics on the efficiency of the proposed structural system was not addressed.

Pall and Marsh [3] also proposed a system in which the frictional devices were incorporated with the braces in a moment resisting frame. It was found that the seismic capacity can be improved and the damage control potential of the frame building can be enhanced by incorporating friction dampers in the bracing system of the building. This device can also be used for enhancing the seismic resistance of existing frame buildings.

Since such systems use bracings and friction joint, there exists a possibility of slip in friction joint before the buckling of brace occurring at a higher load in tension and a lower load in compression. Generally, structural braces are so designed that they act effectively in tension only, i.e. sliding occurs during tension and no sliding takes place during reversal of load. The friction joints with slotted holes can be used to slide in tension or compression, if the brace is designed to avoid buckling in compression till the designed sliding load is attained. Pall [4] has proposed modified sliding friction devices that can be installed at the intersection of steel bracing. These devices aim to solve the drawbacks encountered in the behavior of steel bracing. The sliding of the device, is designed to be restricted under normal loads and moderate earthquake ground motions. During the severe earthquake, the device slides at a predefined load, prior to the occurrence of yielding of structural elements of the frame. However non-sliding phase occurs in the device in every cycle of motion during an actual earthquake, illustrating the inaccuracy of the assumed hysteretic behaviour. At times, buckling of compression brace occurs, whereas tension brace may not slide. Under such conditions, the validity of hysteresis behaviour assumed by Pall and

[1] *Corresponding Author, Former Research Scholar, School of Civil Engineering, KIIT University, Bhubaneswar, Odisha, India, subhransu12930@yahoo.com.*
[2] *Professor, Department of Civil Engineering, Veer Surendra Sai University of Technology, Burla, Odisha, India, litusanjay@yahoo.com*
[3] *Professor, Department of Civil Engineering, IIT, Bombay, Powai, Mumbai, India,rsinha@civil.iitb.ac.in*

Marsh ceases, as the buckled brace will not be pulled back by the mechanism. Therefore, this simple model overestimates the energy dissipation by the friction device. To overcome this situation, a more refined model, by superposing truss and beam-column elements for the diagonal braces, has been developed by Filiatrault and Cherry [5]. This model reflects the more accurate behaviour of the friction damper.

The dissipation of energy in the brace is directly related to the product of sliding force and the slip travelled during each cycle. At a very high force, negligible sliding occurs resulting in negligible dissipation of energy through friction. Similarly, for very low sliding force, the energy dissipation is negligible. Between these two extreme sliding force ranges, there exists an intermediate sliding force value, which gives maximum energy dissipation. However, the ductile behaviour of the structure, which results from the introduction of the friction device, can result in attracting high or low earthquake forces depending on the relationship between structural frequencies and the frequency content of the ground motion. By selecting suitable sliding load, the response of the structure can be adjusted to an optimal value. Filiatrault and Cherry [6 and 7] conducted experimental and analytical studies on the application of the friction device for cross bracing proposed by Pall. They have developed a design spectrum that considers both the characteristics of the structure and ground motion based on their investigation. They [8] also developed specialized algorithms to obtain the optimum slip-load distribution for the friction devices modelled as Coulomb's friction by minimizing a relative performance index (RPI) derived from energy concepts. They have also developed a slip-load spectrum for quick evaluation of optimum slip load. The spectrum takes into account the properties of structure and of the ground motion expected at the location of the structure. From their study an important conclusion was drawn that the optimum slip load depends on the frequency and amplitude of the ground motion and is not strictly dependent on structural properties; also that it is linearly proportional to the peak ground acceleration (PGA). Moreschi [9] and Asahina et al. [10] have followed a genetic algorithm approach to obtain optimum slip-load at the device level and optimal configuration within the frames. The available procedure to obtain an optimum slip-load provides acceptable response reduction to the frame structure. But, the effect of different performance indices (from different response parameters) has not been addressed. The optimum slip-load may be different if the performance index is selected differently.

FitzGerald et al. [11] and Grigorian et al. [12] introduced frictional resistance through slotted bolted connections, which eliminates inelastic member buckling. Slotted Bolted Connection (SBC) is concentric bracing member connections where sliding displacement can occur at a designated friction resistance in long slotted bolt holes. SBC systems have proved to be very efficient in dissipating energy, which is shown through numerous numerical investigations [13 and 14]. Martinez-Rueda [15] proposed the geometry of bracing systems that favour the activation of rotation hysteretic devices at discrete locations of the braces. The adopted geometry eliminates the inconvenience to the designer due to cross-chevron bracings.

The investigations by various researchers indicate that the ratio of the initial sliding load to the yielding force of related structural storey has significant influence on its ability to reduce seismic response [16]. During the development of the friction damper, they have also distinguished the importance of minimization of stick-slide phenomena in order to avoid the introduction of high frequency excitation. The design of these systems relies on accurate modelling of devices and the structural behaviour in the numerical solution process, because of highly nonlinear behaviour.

The dynamic behaviour of friction devices is closely related to the contact theory since there are frictional forces generated by sliding surfaces. In general, the systems involving friction has been idealized as Coulomb's friction in frame structures. In Coulomb's friction model the magnitude of friction is constant at both stick and sliding mode, which is proportional to the force normal to the direction of sliding, and acts opposite to the direction of the sliding velocity. The effectiveness of these systems mostly relies on the modelling of devices and their implementation in the numerical solution process because of their highly nonlinear behaviour. The Coulomb friction system is approximately represented by an equivalent viscous damping system [17]. For friction-based systems Elasto-plastic model is often quite adequate. It has been characterized without a sharp yield point with the use of Bouc and Wen [18] model by a number of researchers. Some investigators have used different equations of the motion for each of the stick and sliding phase [19; 20; 21]. But it has been found that stick and sliding phase can be easily modelled and formulated for single degree of freedom structure, barring the case when a number of vibrating elements are connected by friction dampers, for example in multi-storey buildings. Dimova et al. [22] has simplified the solution process through the special approximation to the Coulomb's friction model. By this approximation they have simplified the mathematical model from non-linear differential equation to a linear differential equation. Levy et al. [23] have developed design methodology for these systems using bilinear hysteretic behaviour. They have presented an algorithm for displacement reversal in the transition from slide to stick. Lyan Ywan Lu et al. [24] has adopted a state-space formulation and a linear integration method to propose a discrete-time solution of dynamic response of a structural system with several friction dampers.

For obtaining the numerical solutions, various researchers have developed computer programs for specific problem while other researchers utilize the available software packages [25] such as DRAIN 2D, DRAIN-2DX, DRAIN-3DX, DRAIN-TABS, DRAIN-BUILDING, SAP2000, ETAB, IDARC 2D, and ADINA. The models used in commercial software packages can be categorised under one of these following two categories:

1. Models where the dynamic behavior of friction devices is modelled by contact analysis theory. This approach can be correct, but expensive in terms of computational effort.
2. Simpler models where Elasto-plastic laws for the friction devices are applied, often as a part of finite element models of the whole structures.

It is observed that numerical solution of differential equation of motion system with friction damper shows high frequency oscillation of relative velocity across sliding surface, when the relative velocity is low (i.e. approaches zero). In these situations the time of phase changeover is not established correctly in the stick-slide model. Identification of the exact time for phase transition is essential for obtaining accurate solutions of equations of motion for dynamic analysis of buildings with friction damper. A numerical methodology for determining the dynamic structural behaviour of the structure with friction damper with improved accuracy has been presented herein. The influence of pretension force and stiffness ratio are also illustrated through an example SDOF system when subjected to ground motions from soft soil, medium soil and hard soil. The paper shows the effect of more precise modelling of friction in the equations of motion.

MATHEMATICAL FORMULATION

Available numerical methodologies to simulate friction behaviour of devices can be divided into different categories. One is equivalent linearization method, in which dissipation due to friction is substituted by an equivalent damping. It is

observed that linearization leads to large displacements during stick phase due to introduction of viscous damping instead of friction force [19]. The second most common approach uses the bilinear model, in which the force-deformation relationship is given in terms of rigid-perfectly plastic idealization [3, 25, 26, 27 and 28]. This approach leads to appropriate results during the first stick phase, but during sliding phase there is deviation in displacement value between computational and experimental results [29]. In third approach, stick-sliding conditions in accordance with the Coulomb friction model [30, 31, 32 and 33] is controlled. Most researchers have presented the modelling for single point of friction contact. Feldstein and Goodman [34] have stated that after only one phase transition between sticking and sliding the local discretization error will be proportional to the first power of the integration step. Many other studies have incorporated the Bouc-Wen model; this model provides continuous transitions from elastic to sliding phases. This model facilitates numerical computation as it does not require the need to track transition phase under arbitrary cyclic motion because of continuous transitions from different phases. Moreover, parameters of this model can be established via a curve fitting procedure from experimental data [35]. As there is no track of change in phase; there will not be a high frequency oscillation in Bouc-Wen model which is the usual case at point of zero velocity with existing stick-sliding numerical simulations. The limitation of Bouc-Wen model is that it requires experimental set up to collect the hysteretic curve parameters if the frictional property varies at its sliding surface.

As the real structures consist of distributed mass and stiffness, hence for the better assessment of their dynamic behaviour, real structures have to be modelled as MDOF systems. From the previous studies it is observed that there exists difficulties, inaccuracy and cost constraints in terms of computational attempt in the formulation of a generalized mathematical method for the determination of the dynamic structural behaviour of the MDOF planar structures equipped with friction damper. An attempt has been made in this paper to formulate a numerical methodology for determining the dynamic structural behaviour of the structure with friction damper with improved accuracy.

Here, the friction surface has been modelled using Coulomb's friction. In this model, the coefficient of friction remains constant and the friction force is expressed as

$$F = F_{st} = F_{sl} = \mu F_N \operatorname{sgn}(\dot{u}) \tag{1}$$

where F is the frictional resistance, which is the same for both stick (F_{st}) and sliding (F_{sl}) stage, μ is the coefficient of friction, F_N is the normal load on the sliding surface, $\dot{u}$ is relative sliding velocity, and sgn($\dot{u}$) is the signum function that assumes a value of +1 for positive sliding velocity and –1 for negative sliding velocity. Two different forces F_{st} and F_{sl} are considered to incorporate different sliding coefficients, if any, in the formulation. This signum function determines the direction of sliding and hence the equation is nonlinear.

The MDOF frame structure with friction slider mounted on Chevron brace (Figure 1) is considered as a two-dimensional (2-D) shear building. Two degrees-of-freedom are present on each floor, resultant to the horizontal displacement of the storey and the brace with damper relative to the ground, as shown in Figure1(a). Simple friction energy-dissipation dampers with slotted bolted connection (SBC) has been considered, where the sliding plate within the vertical plane is connected to the centre line of beam soffit as shown in Figure 1(b). The sliding plate having slotted holes is sandwiched between two clamping plates. The clamping plates are rigidly mounted on the Chevron brace and connected to the sliding plate through pretension bolts. The slotted holes facilitate the sliding of the sliding plate over the frictional interface at constant controllable pretension force. The slotted hole can be of adequate length for the expected slip displacement, and such devices has been widely used in practice.

In this paper, the mathematical formulation of a simplified SDOF system with friction damper, i.e. with a single contact surface, is discussed initially to simplify the understanding of behavioural phase transition (stick to slip/ slide or vice versa) of a single contact friction surface. Then the mathematical formulation of a 2-DOF, i.e. system having two friction dampers, has been derived, which is then extended for formulation of general MDOF system with friction dampers, i.e. with multiple contact surfaces.

Formulation for SDOF System

In the formulation of the SDOF structure the degree-of-freedom of the structure is denoted by subscript *f* and the degrees-of-freedom of the brace with device is denoted by subscript *d*. Two lumped mass models, one for the free frame structure and another for the brace with device, are required to idealize the dynamic behaviour of the structure. The mathematical formulation of a single-degree-of-freedom (SDOF) system having a main frame lumped mass m_{f1}, damping c_{f1}, stiffness k_{f1} and braced frame lumped mass m_{d1}, damping c_{d1}, stiffness k_{d1} have been presented here. The motion consists of two phases: (1) stick phase when the stick friction resistance is not overcome and the structure behaves as conventional braced frame structure, and (2) slip phase when relative motion across the sliding surface between mainframe and device takes place. The overall response consists of series of sliding and non-sliding phases following one another.

Non-Sliding/Stick Phase

During the non-sliding phase, the structure behaves as a conventional fixed base SDOF system. The governing equation of motion at this phase can be expressed as:

$$M\ddot{u}_{f1} + C\dot{u}_{f1} + Ku_{f1} = -M\ddot{u}_g + k_{d1}a_d \tag{2}$$

in which, $M = m_{f1} + m_{d1}$, $C = c_{f1} + c_{d1}$ and $K = k_{f1} + k_{d1}$

$$\ddot{u}_{f1} - \ddot{u}_{d1} = \dot{u}_{f1} - \dot{u}_{d1} = 0, \text{ and } \quad u_{f1} - u_{d1} = a_d \tag{3}$$

$$m_{f1}(\ddot{u}_g + \ddot{u}_{f1}) + c_{f1}\dot{u}_{f1} + k_{f1}u_{f1} < F_s \tag{4}$$

where u_{f1} is the displacement of the top mass (m_{f1}) relative to the ground, u_{d1} is the displacement of the brace mass (m_{d1}) relative to the ground and u_g is the ground displacement. The over dots represent derivative with respect to time while the extent of sliding is represented by a_d. Since the structure is at rest before applying base excitation, the response always starts in stick phase. Therefore, a equals 0 until initiation of first slipping. Stick phase continues up to the initiation of slip phase at every alternative.

Slip Phase

The structure enters into slip phase once the inequality in Eq. (4) is not satisfied and the degree of freedom (DOF) corresponding to the brace becomes independent of floor DOF. As a result, during the slip phase, the structure behaves like a two-degree-of-freedom system. The corresponding equations of motion of the structure and brace mass are given below.

$$m_{f1}\ddot{u}_{f1} + c_{f1}\dot{u}_{f1} + k_{f1}u_{f1} = -m_{f1}\ddot{u}_g - |F|\,\mathrm{sgn}(\dot{u}_{f1} - \dot{u}_{d1}) \quad (5)$$

$$m_{d1}\ddot{u}_{d1} + c_{d1}\dot{u}_{d1} + k_{d1}u_{d1} = -m_{d1}\ddot{u}_g + |F|\,\mathrm{sgn}(\dot{u}_{f1} - \dot{u}_{d1}) \quad (6)$$

$$\mathrm{sgn}(\dot{u}_{f1} - \dot{u}_{d1}) = -\frac{m_{f1}(\ddot{u}_g + \ddot{u}_{f1}) + c_{f1}\dot{u}_{f1} + k_{f1}u_{f1}}{\left|m_{f1}(\ddot{u}_g + \ddot{u}_{f1}) + c_{f1}\dot{u}_{f1} + k_{f1}u_{f1}\right|} \quad (7)$$

where, F is the frictional force in sliding stage (Eq. (1)). The normal force (F_N) for the friction model is from pretension bolts at the joint between device and brace.

Transition Phase

If the sliding velocity during motion becomes zero, the structure may enter into a non-sliding phase or reverse its direction of sliding or have a momentary halt and continue in the same direction. The status of motion during transition phase can be evaluated by checking the validity of Eq. (4) and then applying the corresponding equations of non-sliding or sliding to the next time-step. Any phase may be of very short duration whose results are governed by the transient response and hence very sensitive to the initial conditions. Since the motion in a transition phase acts as initial conditions for subsequent motions, hence the transition point needs to be determined very precisely.

Formulation for MDOF System

The mathematical formulation of multi-degree-of-freedom (MDOF) frame structure with friction slider mounted on Chevron brace (Figure 1) has been presented here in [36]. In the formulation of the MDOF system, the structure degrees-of-freedom is denoted by subscript *f* and the brace with damper degrees-of-freedom by subscript *d*. Two lumped mass models, one for the free frame structure and another for the brace with damper, are required to idealize the dynamic behaviour of the structure.

Through the entire solution process, the equations of motion are split into two subsets with sub-indices *st* representing the non-sliding phase (Stick phase) and *sl* representing the Slip phase (Sliding phase) respectively. The motion of any storey of the structure comprises of either of two phases: (1) non-sliding or stick phase wherein the stick frictional resistance ($\mathbf{F}_{st}$) between the floors and the dampers have not been overcome, and (2) sliding or slip phase in which sliding frictional resistance ($\mathbf{F}_{sl}$) exceeds and the friction force, and acts opposite to the direction of the relative velocity between the floor and friction damper. Linear behaviour of the structure with friction dampers is assumed at both stick and sliding stage of response. The overall response for each storey consists of a series of non-sliding and sliding phases. The number of active degrees of freedom ranges between N (all the dampers in non-sliding phase) and 2N (all dampers are in sliding phase). If the total number of non-sliding floors are denoted by n_{st} and total number of sliding floors n_{sl}, then the total number of degrees of freedom at any instant of time is equal to $n_{st}+2n_{sl}$.

Extending the SDOF formulation, a 2-DOF frame structure with friction slider mounted on Chevron brace (Figure 2(a)) is shown below. The free body diagram showing the lumped masses of the free frame structure and of the brace with damper are shown in Figure 2(b).

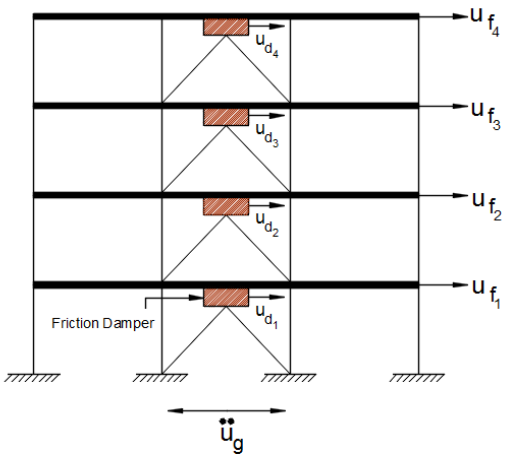

a) Example MDOF system with damper

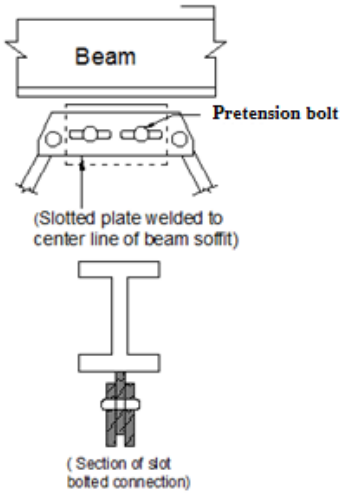

b) Details of friction damper

Figure 1: Schematic diagram of building with friction damper.

As observed from the free body diagram (Figure 2(b)), the equation of motion of the 2-DOF frame structure with friction damper can be given as:

$$\begin{aligned} &m_{f1}(\ddot{u}_{f1} + \ddot{u}_g) + c_{f1}\dot{u}_{f1} + k_{f1}u_{f1} - c_{f2}(\dot{u}_{f2} - \dot{u}_{f1}) \\ &- k_{f2}(u_{f2} - u_{f1}) - c_{d2}(\dot{u}_{d2} - \dot{u}_{f1}) - k_{d2}(u_{d2} - u_{f1}) \\ &+ |F1|\,\mathrm{sgn}(\dot{u}_{f1} - \dot{u}_{d1}) = 0 \end{aligned} \quad (8)$$

$$\begin{aligned} &m_{d1}(\ddot{u}_{d1} + \ddot{u}_g) + c_{d1}\dot{u}_{d1} + k_{d1}u_{d1} \\ &- |F_1|\,\mathrm{sgn}(\dot{u}_{f1} - \dot{u}_{d1}) = 0 \end{aligned} \quad (9)$$

$$\begin{aligned} &m_{f2}(\ddot{u}_{f2} + \ddot{u}_g) + c_{f2}(\dot{u}_{f2} - \dot{u}_{f1}) \\ &+ k_{f2}(u_{f2} - u_{f1}) + |F2|\,\mathrm{sgn}(\dot{u}_{f2} - \dot{u}_{d2}) = 0 \end{aligned} \quad (10)$$

$$\begin{aligned} &m_{d2}(\ddot{u}_{d2} + \ddot{u}_g) + c_{d2}(\dot{u}_{d2} - \dot{u}_{f1}) + \\ &k_{d2}(u_{d2} - u_{f1}) - |F_2|\,\mathrm{sgn}(\dot{u}_{f2} - \dot{u}_{d2}) = 0 \end{aligned} \quad (11)$$

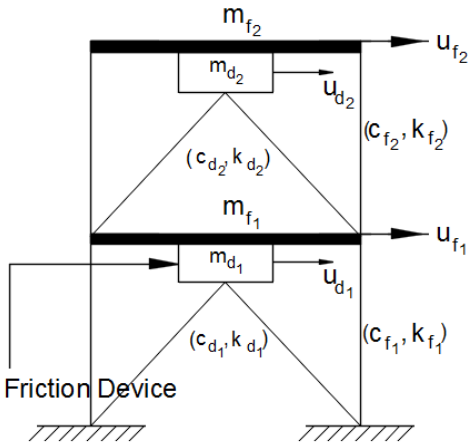

a) 2-DOF structure with damper

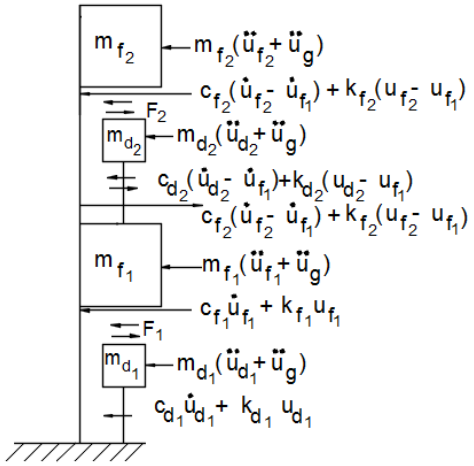

b) Free body diagram of 2DOF system with damper

Figure 2: Schematic diagram of 2DOF system with friction damper.

Rearranging the above in matrix form we get:

$$\begin{bmatrix} m_{f1} & 0 \\ 0 & m_{f2} \end{bmatrix} \times \begin{Bmatrix} \ddot{u}_{f1} \\ \ddot{u}_{f2} \end{Bmatrix} + \begin{bmatrix} c_{f1}+c_{f2}+c_{d2} & -c_{f2} \\ -c_{f2} & c_{f2} \end{bmatrix} \times \begin{Bmatrix} \dot{u}_{f1} \\ \dot{u}_{f2} \end{Bmatrix} +$$
$$\begin{bmatrix} k_{f1}+k_{f2}+k_{d2} & -k_{f2} \\ -k_{f2} & k_{f2} \end{bmatrix} \times \begin{Bmatrix} u_{f1} \\ u_{f2} \end{Bmatrix} + \begin{bmatrix} 0 & -c_{d2} \\ 0 & 0 \end{bmatrix} \times \begin{Bmatrix} \dot{u}_{d1} \\ \dot{u}_{d2} \end{Bmatrix}$$
$$+ \begin{bmatrix} 0 & -k_{d2} \\ 0 & 0 \end{bmatrix} \times \begin{Bmatrix} u_{d1} \\ u_{d2} \end{Bmatrix} = - \begin{bmatrix} m_{f1} & 0 \\ 0 & m_{f2} \end{bmatrix} \times \begin{Bmatrix} 1 \\ 1 \end{Bmatrix} \times \ddot{u}_g - \begin{Bmatrix} F_1 \\ F_2 \end{Bmatrix} \quad (12)$$

and

$$\begin{bmatrix} m_{d1} & 0 \\ 0 & m_{d2} \end{bmatrix} \times \begin{Bmatrix} \ddot{u}_{d1} \\ \ddot{u}_{d2} \end{Bmatrix} + \begin{bmatrix} c_{d1} & 0 \\ 0 & c_{d2} \end{bmatrix} \times \begin{Bmatrix} \dot{u}_{d1} \\ \dot{u}_{d2} \end{Bmatrix}$$
$$+ \begin{bmatrix} k_{d1} & 0 \\ 0 & k_{d2} \end{bmatrix} \times \begin{Bmatrix} u_{d1} \\ u_{d2} \end{Bmatrix} + \begin{bmatrix} 0 & 0 \\ -c_{d2} & 0 \end{bmatrix} \times \begin{Bmatrix} \dot{u}_{f1} \\ \dot{u}_{f2} \end{Bmatrix}$$
$$+ \begin{bmatrix} 0 & 0 \\ -k_{d2} & 0 \end{bmatrix} \times \begin{Bmatrix} u_{f1} \\ u_{f2} \end{Bmatrix} = - \begin{bmatrix} m_{d1} & 0 \\ 0 & m_{d2} \end{bmatrix} \times \begin{Bmatrix} 1 \\ 1 \end{Bmatrix} \times \ddot{u}_g + \begin{Bmatrix} F_1 \\ F_2 \end{Bmatrix} \quad (13)$$

Eq. 12 and Eq. 13 can further be rearranged in a matrix form as:

$$\begin{bmatrix} m_{f1} & 0 & 0 & 0 \\ 0 & m_{f2} & 0 & 0 \\ 0 & 0 & m_{d1} & 0 \\ 0 & 0 & 0 & m_{d2} \end{bmatrix} \times \begin{Bmatrix} \ddot{u}_{f1} \\ \ddot{u}_{f2} \\ \ddot{u}_{d1} \\ \ddot{u}_{d2} \end{Bmatrix} +$$
$$\begin{bmatrix} (c_{f1}+c_{f2})+c_{d2} & -c_{f2} & 0 & -c_{d2} \\ -c_{f2} & c_{f2} & 0 & 0 \\ 0 & 0 & c_{d1} & 0 \\ -c_{d2} & 0 & 0 & c_{d2} \end{bmatrix} \times \begin{Bmatrix} \dot{u}_{f1} \\ \dot{u}_{f2} \\ \dot{u}_{d1} \\ \dot{u}_{d2} \end{Bmatrix}$$
$$+ \begin{bmatrix} (k_{f1}+k_{f2})+k_{d2} & -k_{f2} & 0 & -k_{d2} \\ -k_{f2} & k_{f2} & 0 & 0 \\ 0 & 0 & k_{d1} & 0 \\ -k_{d2} & 0 & 0 & k_{d2} \end{bmatrix} \times \begin{Bmatrix} u_{f1} \\ u_{f2} \\ u_{d1} \\ u_{d2} \end{Bmatrix}$$
$$= - \begin{bmatrix} m_{f1} & 0 & 0 & 0 \\ 0 & m_{f2} & 0 & 0 \\ 0 & 0 & m_{d1} & 0 \\ 0 & 0 & 0 & m_{d2} \end{bmatrix} \times \begin{Bmatrix} 1 \\ 1 \\ 1 \\ 1 \end{Bmatrix} \times \ddot{u}_g + \begin{Bmatrix} F_1 \\ F_2 \\ -F_1 \\ -F_2 \end{Bmatrix} \quad (14)$$

In matrix form, Eq.14 can be expressed as:

$$\begin{bmatrix} \mathbf{M}_f & \mathbf{0} \\ \mathbf{0} & \mathbf{M}_d \end{bmatrix} \times \begin{Bmatrix} \ddot{\mathbf{u}}_f \\ \ddot{\mathbf{u}}_d \end{Bmatrix} + \begin{bmatrix} \mathbf{C}_f + \mathbf{C}_{d2} & \mathbf{C}_{d3} \\ (\mathbf{C}_{d3})^T & \mathbf{C}_{d1} \end{bmatrix} \times \begin{Bmatrix} \dot{\mathbf{u}}_f \\ \dot{\mathbf{u}}_d \end{Bmatrix}$$
$$+ \begin{bmatrix} \mathbf{K}_f + \mathbf{K}_{d2} & \mathbf{K}_{d3} \\ (\mathbf{K}_{d3})^T & \mathbf{K}_{d1} \end{bmatrix} \times \begin{Bmatrix} \mathbf{u}_f \\ \mathbf{u}_d \end{Bmatrix} = - \begin{bmatrix} \mathbf{M}_f & \mathbf{0} \\ \mathbf{0} & \mathbf{M}_d \end{bmatrix} \times \begin{Bmatrix} \mathbf{r}_f \\ \mathbf{r}_d \end{Bmatrix} \times \ddot{\mathbf{u}}_g - \begin{Bmatrix} +\mathbf{F}_f \\ -\mathbf{F}_f \end{Bmatrix} \quad (15)$$

where,

$$\mathbf{M}_f = \begin{bmatrix} m_{f1} & 0 \\ 0 & m_{f2} \end{bmatrix}, \mathbf{M}_d = \begin{bmatrix} m_{d1} & 0 \\ 0 & m_{d2} \end{bmatrix},$$
$$\mathbf{C}_f = \begin{bmatrix} c_{f1}+c_{f2} & -c_{f2} \\ -c_{f2} & c_{f2} \end{bmatrix}, \mathbf{C}_{d2} = \begin{bmatrix} c_{d2} & 0 \\ 0 & 0 \end{bmatrix}, \mathbf{C}_{d3} = \begin{bmatrix} 0 & -c_{d2} \\ 0 & 0 \end{bmatrix},$$
$$\mathbf{K}_f = \begin{bmatrix} k_{f1}+k_{f2} & -k_{f2} \\ -k_{f2} & k_{f2} \end{bmatrix}, \mathbf{K}_{d2} = \begin{bmatrix} k_{d2} & 0 \\ 0 & 0 \end{bmatrix}, \mathbf{K}_{d3} = \begin{bmatrix} 0 & -k_{d2} \\ 0 & 0 \end{bmatrix},$$
$$\mathbf{u}_f = \begin{Bmatrix} u_{f1} \\ u_{f2} \end{Bmatrix}, \mathbf{u}_d = \begin{Bmatrix} u_{d1} \\ u_{d2} \end{Bmatrix}, \mathbf{r}_f = \mathbf{r}_d = \begin{Bmatrix} 1 \\ 1 \end{Bmatrix}, \quad \mathbf{F}_f = \begin{Bmatrix} F_1 \\ F_2 \end{Bmatrix} \quad (16)$$

The equations of motion for the 2-DOF system, as shown in Eq.15 can also be represented as

$$\mathbf{M}\ddot{\mathbf{u}} + \mathbf{C}\dot{\mathbf{u}} + \mathbf{K}\mathbf{u} = -\mathbf{M}\mathbf{r}\ddot{u}_g - \mathbf{F} \quad (17)$$

where,

$$\mathbf{M}=\begin{bmatrix}\mathbf{M}_f & \mathbf{0}\\ \mathbf{0} & \mathbf{M}_d\end{bmatrix},\mathbf{C}=\begin{bmatrix}\mathbf{C}_f+\mathbf{C}_{d2} & \mathbf{C}_{d3}\\ (\mathbf{C}_{d3})^T & \mathbf{C}_{d1}\end{bmatrix},$$
$$\mathbf{K}=\begin{bmatrix}\mathbf{K}_f+\mathbf{K}_{d2} & \mathbf{K}_{d3}\\ (\mathbf{K}_{d3})^T & \mathbf{K}_{d1}\end{bmatrix},\mathbf{u}=\begin{Bmatrix}\mathbf{u}_f\\ \mathbf{u}_d\end{Bmatrix},\dot{\mathbf{u}}=\begin{Bmatrix}\dot{\mathbf{u}}_f\\ \dot{\mathbf{u}}_d\end{Bmatrix},\ddot{\mathbf{u}}=\begin{Bmatrix}\ddot{\mathbf{u}}_f\\ \ddot{\mathbf{u}}_d\end{Bmatrix},$$
$$\mathbf{r}=\begin{Bmatrix}\mathbf{r}_f\\ \mathbf{r}_d\end{Bmatrix},\mathbf{r}_f=\mathbf{r}_d=\begin{Bmatrix}1\\ 1\end{Bmatrix}\ and\ \ \mathbf{F}=\begin{Bmatrix}+\mathbf{F}_f\\ -\mathbf{F}_f\end{Bmatrix} \tag{18}$$

The equations of motion for 2-DOF system, as shown in Eq.17, can be generalised for MDOF system (having *'n'* DOF) in matrix form and can be represented as:

$$\mathbf{M}\ddot{\mathbf{u}}_{st+sl}+\mathbf{C}\dot{\mathbf{u}}_{st+sl}+\mathbf{K}\mathbf{u}_{st+sl}=-\mathbf{M}\mathbf{r}\ddot{u}_g-\mathbf{F}_{f+sl} \tag{19}$$

where **M**, **C**, and **K** are mass, damping and stiffness matrices, respectively, **r** is the force-influence vector, **u** represents the displacement degrees of freedom relative to the base of the structure and u_g is the base displacement. The over dots represent derivatives with respect to time, i.e. $\ddot{\mathbf{u}}_{st+sl}$ represents the acceleration relative to the base, $\ddot{u}_g$ represents the ground acceleration and $\dot{\mathbf{u}}_{st+sl}$ represents the floor velocity relative to the base. The friction force vector is represented as **F**, and the matrices are given as:

$$\mathbf{u}_{st+sl}=\begin{Bmatrix}\mathbf{u}_{f,st+sl}\\ \mathbf{u}_{d,st+sl}\end{Bmatrix},\mathbf{r}=\begin{Bmatrix}\mathbf{r}_f\\ \mathbf{r}_d\end{Bmatrix},\mathbf{F}=\begin{Bmatrix}+\mathbf{F}_{f+sl}\\ -\mathbf{F}_{f+sl}\end{Bmatrix} \tag{20}$$

where

$$\mathbf{M}_d=\begin{bmatrix}m_{d1} & 0 & 0\\ 0 & \ddots & 0\\ 0 & 0 & m_{dN}\end{bmatrix},$$
$$\mathbf{C}_{d1}=\begin{bmatrix}c_{d1} & 0 & 0\\ 0 & \ddots & 0\\ 0 & 0 & c_{dN}\end{bmatrix},\mathbf{C}_{d2}=\begin{bmatrix}c_{d2} & 0 & 0\\ 0 & \ddots & c_{dN}\\ 0 & 0 & 0\end{bmatrix},\mathbf{C}_{d3}=\begin{bmatrix}0 & -c_{d2} & 0\\ 0 & 0 & \ddots\\ 0 & 0 & -c_{dN}\end{bmatrix},$$
$$\mathbf{K}_{d1}=\begin{bmatrix}k_{d1} & 0 & 0\\ 0 & \ddots & 0\\ 0 & 0 & k_{dN}\end{bmatrix},\mathbf{K}_{d2}=\begin{bmatrix}k_{d2} & 0 & 0\\ 0 & \ddots & k_{dN}\\ 0 & 0 & 0\end{bmatrix},\mathbf{K}_{d3}=\begin{bmatrix}0 & -k_{d2} & 0\\ 0 & 0 & \ddots\\ 0 & 0 & -k_{dN}\end{bmatrix} \tag{21}$$

In the above equations, $\mathbf{M}_f$, $\mathbf{C}_f$ and $\mathbf{K}_f$ are the N ×N mass, damping and stiffness matrices of the structure excluding the bracing members. $\mathbf{M}_d$, $\mathbf{C}_{d1}$, $\mathbf{C}_{d2}$, $\mathbf{C}_{d3}$, $\mathbf{K}_{d1}$, $\mathbf{K}_{d2}$ and $\mathbf{K}_{d3}$ are N ×N mass, damping and stiffness matrices of the brace with friction damper, respectively. The damping property of the free frame (excluding the brace with damper) structure may be different from the same of the brace with damper. So the complete structure is non-classical damped system. The non-classical damping matrix [C] for the structure is developed by first evaluating the classical damping matrix for the free frame, [$\mathbf{C}_f$], based on the damping ratios appropriate for the structure [37].

The structure and the brace DOFs at any storey satisfy the following conditions during the stick phase:

$$\ddot{\mathbf{u}}_{f,st}=\ddot{\mathbf{u}}_{d,st}$$
$$\dot{\mathbf{u}}_{f,st}=\dot{\mathbf{u}}_{d,st} \tag{22}$$
$$\mathbf{u}_{f,st}-\mathbf{u}_{d,st}=\text{constant}$$

In Eq. (19), stick or non-sliding phase of a particular floor requires that the corresponding friction force satisfy the equation,

$$\left|\mathbf{F}_f\right|<\mathbf{F}_{st} \tag{23}$$

where the friction force vector, consisting of friction force in all the dampers can be given by:

$$\mathbf{F}_f=\mathbf{M}_{f,st}\ddot{\mathbf{u}}_{f,st+sl}+\mathbf{M}_{f,st}\mathbf{r}_f\ddot{u}_g+(\mathbf{C}_{f,st}+\mathbf{C}_{d2,st})\dot{\mathbf{u}}_{f,st+sl}+$$
$$\mathbf{C}_{d3,st}\dot{\mathbf{u}}_{d,st+sl}+(\mathbf{K}_{f,st}+\mathbf{K}_{d2,st})\mathbf{u}_{f,st+sl}+\mathbf{K}_{d3,st}\mathbf{u}_{d,st+sl} \tag{24}$$

In Eq. (24), $\mathbf{F}_f$ is the vector of frictional resistance of all friction dampers at stick stage. When the inequality in Eq. (23) is not satisfied for any floor, that floor enters into the sliding phase. Then the corresponding brace degree-of-freedom at the floor level also becomes active in the equations of motion.

The direction of sliding of a brace degree of freedom can be expressed by the following relationship:

$$\text{sgn}(\dot{u}_f-\dot{u}_d)=-\frac{F_{f\,max}}{\left|F_{f\,max}\right|} \tag{25}$$

The response of the structure always starts from rest in stick phase. This phase of response continues until the unbalanced frictional resistance of any floor exceeds the maximum frictional resistance of the brace with damper at that floor. It is important to note that the number of storey experiencing stick and sliding conditions varies continuously through the entire response phase. When the relative sliding velocity ($\dot{u}_f-\dot{u}_d$) at any floor becomes zero or changes its sign during motion, then the brace with damper at that storey may enter the stick phase/ or non-sliding phase. It may also reverse its course of sliding or have a temporary halt and maintain the direction of sliding. The status of motion during transition phase can be evaluated from Eq. (26). The equations of motion corresponding to the appropriate stick or sliding phase are evaluated during the next time-step.

SOLUTION PROCEDURE

The complete solution consists of a series of non-sliding (stick) and sliding phases at each storey level following one to another which makes the system highly nonlinear. Appropriate nonlinear solution techniques can be adopted for solving these nonlinear equations. Among the many methods one of the most effective is the step-by-step direct integration method. The authors have used a modification of step-by-step linear acceleration method. The correctness of the result is very sensitive to the alteration in phase of motion from stick phase to slip phase and vice versa, throughout the solution of such nonlinear equations. This can be addressed by sub-dividing the selected time interval whenever change of phase occurs. This can be possible for single point sliding system, but for multi-point sliding system this approach will be very complex. In the present study, the response is evaluated at successive increment Δt (10^{-6} second) of time, usually equal length of time is considered for computational convenience.

At the beginning of each interval, the condition of dynamic equilibrium is established.

The equations of motion in matrix form at a particular i^{th} time step can be divided into two equations: (1) equations at the degrees-of-freedom on the level of the floors, and (2) equations at the degrees-of-freedom on the level of dampers. The response at i+1 time step can be computed from the

known response at the i^{th} time step. It is initially assumed that the sticking-sliding conditions in the damper at the instant i are the same at i+1. The complete solution consists of three nested iteration loops with coupling quantities i.e. $\mathbf{u}_{f,i+1}$, $\mathbf{u}_{d,i+1}$, $\dot{\mathbf{u}}_{f,i+1}$, $\dot{\mathbf{u}}_{d,i+1}$ and $\mathbf{F}_{f,i+1}$ and the estimated unbalanced frictional resistance $\left(\mathbf{F}_{f,st,i+1}\right)_{temp}$ as well as estimated acceleration $\left(\left(\ddot{\mathbf{u}}_{f,i+1}\right)_{temp},\left(\ddot{\mathbf{u}}_{d,i+1}\right)_{temp}\right)$ at time step i+1. Initially at i+1 floor displacement, damper displacement, floor velocity, damper velocity with assumed initial estimated quantities of floor and damper acceleration can be obtained. The *'temp' variables* are introduced in the alogorithm in order to store the response quantities obtained in a particular iteration step and to verify whether the response quantity obtained in that iteration is matching with the previously calculated/known value. In case of disagreement in values of response quantities for i^{th} and $(i+1)^{th}$ time step, the value stored in the '*temp' variable* at the end of the previous iteration ($(i+1)^{th}$ time step) is considered as the calculated/ known value for the next iteration ($(i+2)^{th}$ time step) and consequently the values of '*temp' variable* is updated for that iteration step.

The equations of motion is split into two subsets with sub-indices '*st'* representing non-sliding or stick phase and *'sl'* representing slip or sliding phase. If n_{st} is the total number of non-sliding (stick) floors and N is the total number of floors, then n_{sl}, i.e. the total number of sliding floors is equal to $(N-n_{st})$. Further Eq. (19 and 20) can be represented as

$$\mathbf{M}_f(\ddot{\mathbf{u}}_{f,st+sl})+\mathbf{C}_{d3}(\dot{\mathbf{u}}_{d,st+sl})+[\mathbf{C}_f+\mathbf{C}_{d2}](\dot{\mathbf{u}}_{f,st+sl})+ [\mathbf{K}_f+\mathbf{K}_{d2}](\mathbf{u}_{f,st+sl})+[\mathbf{K}_{d3}](\mathbf{u}_{d,st+sl})=-\mathbf{M}_f\mathbf{r}_f\ddot{u}_g-\mathbf{F}_{f+sl} \quad (26)$$

and

$$\mathbf{M}_d(\ddot{\mathbf{u}}_{d,st+sl})+[\mathbf{C}_{d3}]^T(\dot{\mathbf{u}}_{f,st+sl})+[\mathbf{C}_{d1}](\dot{\mathbf{u}}_{d,st+sl})+ [\mathbf{K}_{d3}]^T(\mathbf{u}_{f,st+sl})+[\mathbf{K}_{d1}](\mathbf{u}_{d,st+sl})=-\mathbf{M}_d\mathbf{r}_d\ddot{u}_g+\mathbf{F}_{f+sl} \quad (27)$$

where, for non-sliding or stick floors (n_{st})

$$(\mathbf{u}_{f,st})=[\mathbf{u}_{f1,st},\mathbf{u}_{f2,st},\mathbf{u}_{f3,st},.....\mathbf{u}_{fn_{st},st}]^T$$
$$(\mathbf{u}_{d,st})=[\mathbf{u}_{d1,st},\mathbf{u}_{d2,st},\mathbf{u}_{d3,st},.....\mathbf{u}_{fn_{st},st}]^T \quad (28)$$

and for sliding floors (n_{sl})

$$(\mathbf{u}_{f,sl})=[\mathbf{u}_{f1,sl},\mathbf{u}_{f2,sl},\mathbf{u}_{f3,sl},.....\mathbf{u}_{fn_{sl},sl}]^T$$
$$(\mathbf{u}_{d,sl})=[\mathbf{u}_{d1,sl},\mathbf{u}_{d2,sl},\mathbf{u}_{d3,sl},.....\mathbf{u}_{dn_{sl},sl}]^T \quad (29)$$

$\dot{\mathbf{u}}_{f,st+sl}$, $\dot{\mathbf{u}}_{d,st+sl}$, $\ddot{\mathbf{u}}_{f,st+sl}$ and $\ddot{\mathbf{u}}_{d,st+sl}$ can be arranged in the similar pattern.

It is pertinent to note that number of non-sliding floors (n_{st}) and number of sliding floors (n_{sl}) vary continuously through the entire time history analysis. The solution algorithm followed in the current paper is discussed as below.

As per the Newmark's step-by-step direct integration method,

$$[\dot{\mathbf{u}}_{f,st+sl}]_{i+1}=[\dot{\mathbf{u}}_{f,st+sl}]_i+(1-\gamma)\Delta t[\ddot{\mathbf{u}}_{f,st+sl}]_i+\gamma\Delta t[\ddot{\mathbf{u}}_{f,st+sl}]_{i+1} \quad (30)$$

$$[\mathbf{u}_{f,st+sl}]_{i+1}=[\mathbf{u}_{f,st+sl}]_i+\Delta t[\dot{\mathbf{u}}_{f,st+sl}]_i+(0.5-\beta)\Delta t^2[\ddot{\mathbf{u}}_{f,st+sl}]_i+\beta\,\Delta t^2[\ddot{\mathbf{u}}_{f,st+sl}]_{i+1} \quad (31)$$

$$[\dot{\mathbf{u}}_{d,st}]_{i+1}=[\dot{\mathbf{u}}_{f,st}]_{i+1} \quad (32)$$

$$[\dot{\mathbf{u}}_{d,sl}]_{i+1}=[\dot{\mathbf{u}}_{d,sl}]_i+(1-\gamma)\Delta t[\ddot{\mathbf{u}}_{d,sl}]_i+\gamma\Delta t[\ddot{\mathbf{u}}_{d,sl}]_{i+1} \quad (33)$$

$$[\mathbf{u}_{d,st}]_{i+1}=[\mathbf{u}_{d,st}]_i+\{[\mathbf{u}_{f,st}]_{i+1}-[\mathbf{u}_{f,st}]_i\} \quad (34)$$

$$[\mathbf{u}_{d,sl}]_{i+1}=[\mathbf{u}_{d,sl}]_i+\Delta t[\dot{\mathbf{u}}_{d,sl}]_i+(0.5-\beta)\Delta t^2[\ddot{\mathbf{u}}_{d,sl}]_i+\beta\,\Delta t^2[\ddot{\mathbf{u}}_{d,sl}]_{i+1} \quad (35)$$

The values of integration parameters "γ" and "β*"* can be considered as γ = ½ and β = ¼ for average acceleration method and γ = ½ and β = ⅙ for linear acceleration method. These above equations (i.e. Eq. (30) to Eq. (35)) combined with the equilibrium equations, i.e. Eq. (19), Eq. (26) and Eq. (27) provide the basis for computing $[\mathbf{u}_{f,st+sl}]$, $[\mathbf{u}_{d,st+sl}]$, $[\dot{\mathbf{u}}_{f,st+sl}]$, $[\dot{\mathbf{u}}_{d,st+sl}]$, $[\ddot{\mathbf{u}}_{f,st+sl}]$ and $[\ddot{\mathbf{u}}_{d,st+sl}]$ at time step (i+1) from the known quantities at time *i*, at the end of each time step. Then further iteration is required to implement these computations because the unknown response quantities at time (i+1) appear in the right hand side of the equations (i.e. Eq. (30) to Eq. (35)). To start the iteration, it is assumed that the response at instant (i+1) is the same at that at instant *i.*

At first iteration loop, acceleration at all the floors relative to the base can be computed from Eq. (26), as below

where,

$$\ddot{\mathbf{u}}_{f,st+sl}=(\mathbf{M}_f)^{-1}[-(\mathbf{C}_f+\mathbf{C}_{d2})(\dot{\mathbf{u}}_{f,st+sl})_{i+1}-\mathbf{C}_{d3}(\dot{\mathbf{u}}_{d,st+sl})_{i+1}-(\mathbf{K}_f+\mathbf{K}_{d2})(\mathbf{u}_{f,st+sl})_{i+1}-\mathbf{K}_{d3}(\mathbf{u}_{d,st+sl})_{i+1}-\mathbf{M}_f\mathbf{r}_f\ddot{u}_g-\mathbf{F}_{f+sl}] \quad (36)$$

In the second iteration loop, the unbalanced frictional resistance at all the non-sliding floors (n_{st}) can be computed from Eq.(27) using "n_{st}" equations as below,

$$[\mathbf{F}_f]_{i+1}=\mathbf{M}_{d,st}(\ddot{\mathbf{u}}_{d,st+sl})_{i+1}+[\mathbf{C}_{d3,st}]^T(\dot{\mathbf{u}}_{f,st+sl})_{i+1}+\mathbf{C}_{d1,st}(\dot{\mathbf{u}}_{d,st+sl})_{i+1} +[\mathbf{K}_{d3,st}]^T(\mathbf{u}_{f,st+sl})_{i+1}+\mathbf{K}_{d1,st}(\mathbf{u}_{d,st+sl})_{i+1}+\mathbf{M}_{d,st}\mathbf{r}_d(\ddot{\mathbf{u}}_g)_{i+1} \quad (37)$$

In the third iteration loop, acceleration of the brace with damper can be calculated for all the sliding floors (n_{sl}), from the Eq. (27) using n_{sl} equations as below,

$$[\ddot{\mathbf{u}}_{d,sl}]_{i+1}=(\mathbf{M}_{d,sl})^{-1}[-(\mathbf{C}_{d3,sl})^T(\dot{\mathbf{u}}_{f,st+sl})_{i+1}-\mathbf{C}_{d1,sl}(\dot{\mathbf{u}}_{d,st+sl})_{i+1} -(\mathbf{K}_{d3,sl})^T(\mathbf{u}_{f,st+sl})_{i+1}-\mathbf{K}_{d1,sl}(\mathbf{u}_{d,st+sl})_{i+1}-\mathbf{M}_{d,sl}\mathbf{r}_d(\ddot{u}_g)_{i+1}+\mathbf{F}_{sl}] \quad (38)$$

Iterations will continue until the convergence to the tolerance error (10^{-6}) between new and old estimated quantities. Thus, after the fulfilment of the established conditions for the above iteration loops, the sliding-sticking condition Eq. (23) at the each floor level must be checked before going to the next instant. The detail solution procedure is presented in the flow chart shown in Figure 3.

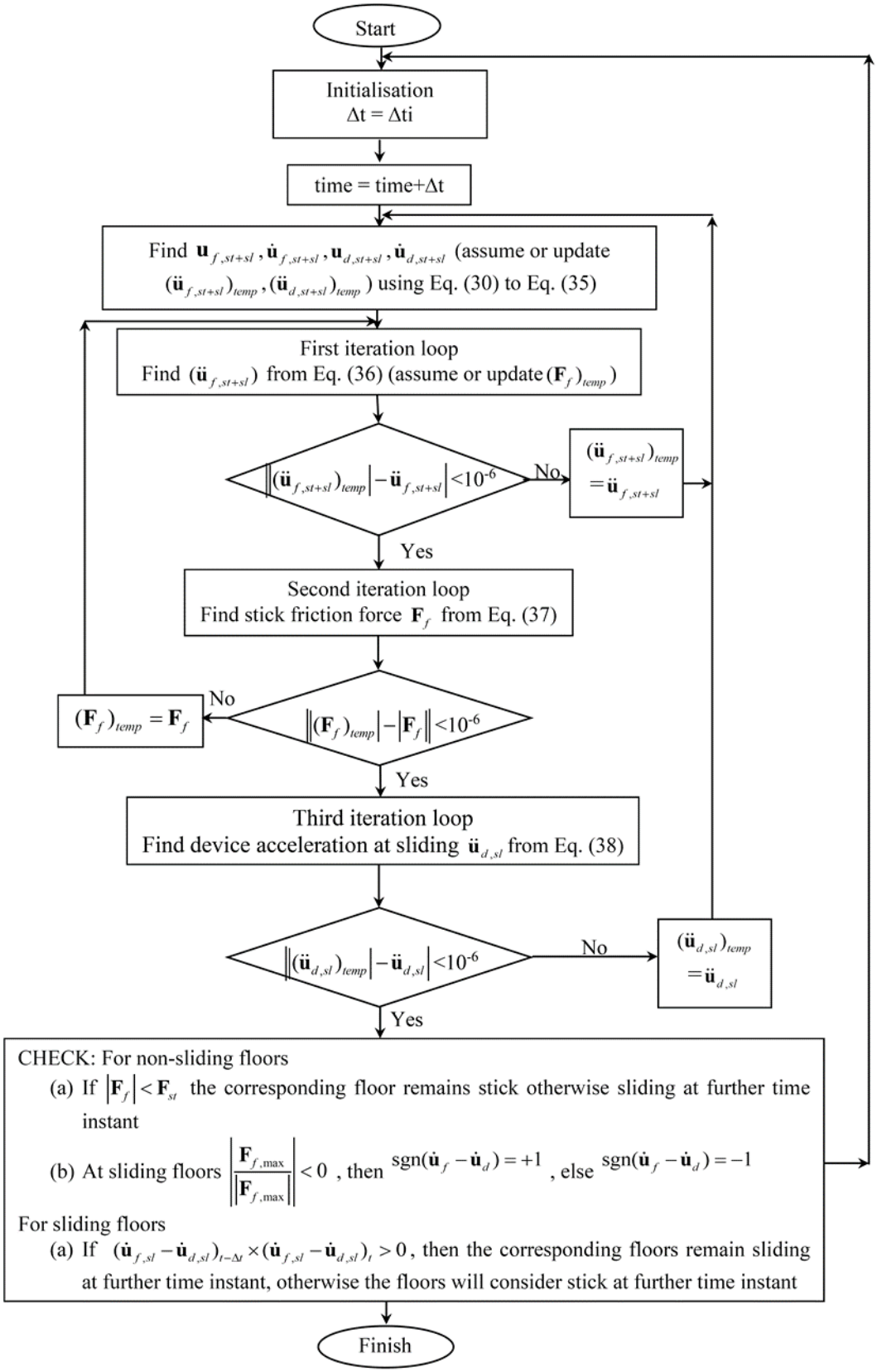

Figure 3: Flow chart showing solution process.

VALIDATION PROBLEMS

The results obtained from the proposed method using FORTRAN code have been compared with that from published results to ascertain the validity and accuracy of the methodology. To verify the accuracy of the proposed methodology for single degree of freedom system the results obtained using the proposed methodology for an example frame with K bracings, subjected to seismic loading, have been compared with the published results [22]. Similarly, existing code has been validated for MDOF problem with friction dampers by comparing the displacement time history response of a braced frame with friction dampers, obtained from the proposed method with the results obtained by Dimova et al. [22] for the example MDOF braced frame with friction damper when subjected to seismic excitation.

Single Storey Frame with K Bracings (i.e. SDOF System)

From the published literature the single storey frame with K bracing with a friction joint with slotted holes, termed as additional frame has been considered for validation of the proposed method. The single storey frame has the following characteristics: length of beam (l) = 6.1m, height of columns (h) = 3.5 m, mass of the frame (m_1) = 20,000 kg, the mass of the additional frame (m_2) = 27 kg, the natural period of the main frame is 0.4 sec and the natural period of the additional frame is 0.0684 sec. The coefficient of friction is assumed to be 0.15. The structural damping is taken as 2%. The seismic excitation is given by a NS component of the accelerogram recorded at the Kalamata/Greece earthquake of 13 September 1986, discretized in steps of 0.00976 with peak ground acceleration of 0.240g.

To validate the proposed methodology, the equations of motion in stick phase and sliding phase have been solved by step by step direct integration method. The displacement response of the additional frame with respect to time has been obtained using the code developed. To represent the small value of the relative velocity between the mainframe and the additional frame three error tolerance limits for relative velocity (i.e. 0.001, 0.005 and 0.01) were considered by Dimova for estimating the influence of friction force approximation on the solution accuracy. In the current stick slip method as the relative velocity has influence in determining the direction of motion of the device only and not considered for approximation of friction force, hence, no particular error tolerance limit has been considered in the present approach. The results obtained from the present method is plotted along with the displacement Time history for the different approximations of the friction force for the additional frame from published work [22], as shown in Figure4.

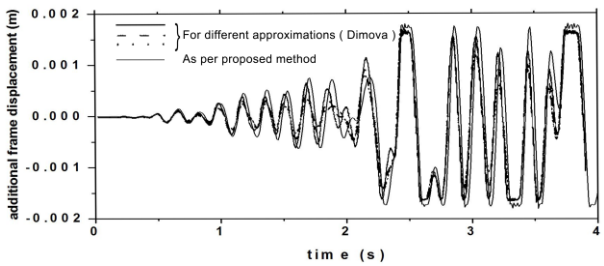

Figure 4: Displacement Time history for different approximations of the friction force for the additional frame from published work [22] and using the proposed method.

From these results it is clear that the result plot obtained from the proposed method is in close agreement with the published result plots. The published results are verified by experimental studies. Hence, the response behaviour of the system using the proposed method can be in close agreement with the expected physical behaviour.

Four Storey Steel Frame with Friction Damper (i.e. MDOF Frame with Friction Damper)

The four storey steel frame with friction damper, considered by Dimova et al. [22] has been considered for evaluating the validation and accuracy of the proposed method in analysing the for MDOF frame with friction dampers subjected to base excitations. The four storey steel frame, as shown in Figure 5 has the following characteristics: Storey masses $m_1 = m_2 = m_3$ = 41,610 kg, m_4 = 40,820 kg, bracing masses $m_1' = m_2' = m_3'$ = m_4' = 23 kg the first natural period of the initial moment resisting frame is 1.006 s and the natural period of the braced frame is 0.612 s. The coefficient of friction has been assumed to be 0.15. The structural damping has been taken as 2%. The seismic excitation considered is given by a NS component of the accelerogram recorded at the Kalamata/Greece earthquake of 13 September 1986, discretized in steps of 0.00976 with peak ground acceleration of 0.240g. For the analysis purpose the ordinates at consecutive time step are averaged to get a third central ordinate so that the formulation can be applied without any difficulty. The satisfaction of this equation decides the degree of the accuracy. Although the solution of equations of motion themselves may not require a very small time step, a time step of the order of 1×10^{-6} sec is considered to get results with acceptable accuracy.

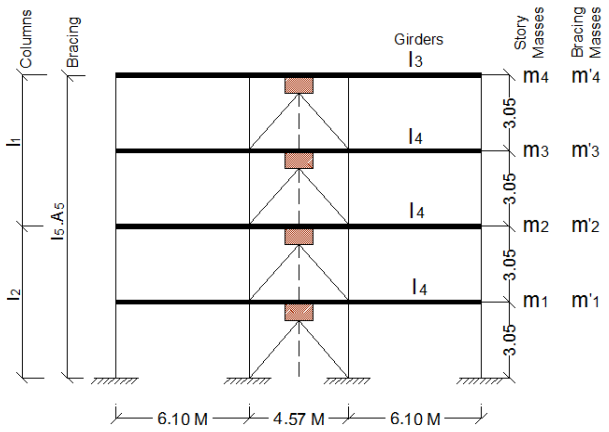

Figure 5: Four storey steel frame with friction devices [22].

The displacement time history response obtained from the analysis for the four storey moment resisting steel frame and four storey steel frame with friction device, using the proposed method has been compared with the published literature as shown in Figure 6. From these results it is clear that the proposed analysis results are in complete agreement with the published solution.

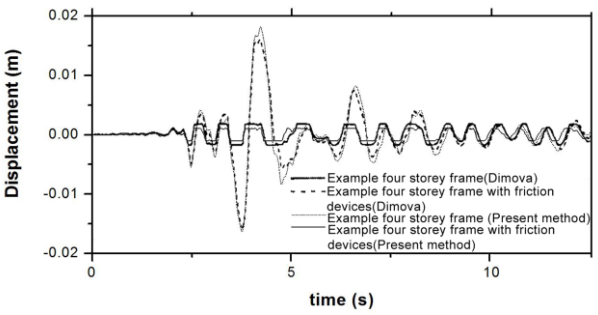

Figure 6: Displacement Time history for the additional frame from published work [22] and using the proposed method.

EXAMPLE APPLICATION

From the results of validation problems it is seen that the proposed methodology successfully estimates the expected physical behaviour of the structure with friction damper due to more precise modelling of friction in the equtions of motion. The relative advantage of friction damper depends on stiffness ratio and pretension force. The extent of influence of these factors on the seismic performance of friction damper in a SDOF system with friction device (Figure 7) has been investigated in this chapter using the proposed methodology. Friction joints with slotted holes are positioned in such a manner that sliding plate can be mounted vertically as shown in Figure 7 (b). The placement of sliders in vertical plane of the beam ensures that only the pretension force controls the normal load on the sliding surface. The presence of two friction interfaces doubles the frictional resistance. The total normal load (F_N) on the sliding surface is equal to $2n_b F_{Ni}$, where n_b is the number of pretension bolts, and F_{Ni} is the pretension force in a single bolt. All the bolts in a particular friction device are assumed to have the same pretension force. It may be noted that the structure weight does not have any effect of the normal load (F_N). The value of the coefficient of friction has been considered for steel on steel slider as per Indian standard code of practice i.e. μ = 0.5. The braces with damping devices exhibit highly nonlinear behaviour. The effect of energy dissipation due to viscous damping in the brace members is normally very small compared to the work done by friction sliding. So the viscous damping in brace has been neglected. The structural damping ratio of the free-frame has been taken as 5% of its critical damping. The frame is represented as a lumped mass model with lumped masses of 20000 kg and 50 kg for frame and brace respectively.

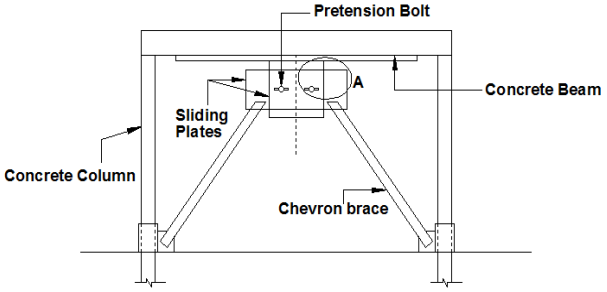

a) Example Structure

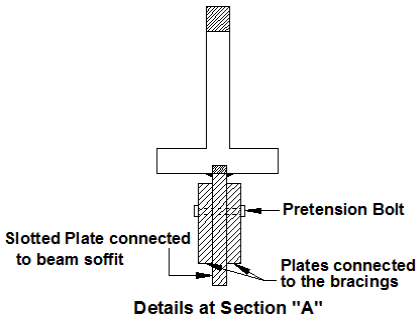

b) Details of friction damper

Figure 7: SDOF structural model with friction device.

The characteristics of ground motion that are important are peak ground accelerations (PGA), duration of strong motion, and its frequency content. The ground motions chosen in this investigation cover a wide variety of earthquakes having different peak ground accelerations, frequency composition and duration. A total of nine different earthquake ground motions have been used based on the soil type and their details are given in Table.1. These records are categorized in three groups based on the soil type at the recording stations, and their time-histories are shown in Figure 8. Three time histories have been selected for each of soft soil (FSR1, FSR2 and FSR3), alluvium or medium soil (FMR1, FMR2 and FMR3) and hard soil or rock (FHR1, FHR2 and FHR3). The evaluations using these ground motions represent the likely response under the likely range of expected ground motion characteristics. The ensemble of spectral acceleration of ground motion records is presented at Figure 9.

Table 1: Details of ground motion records used for numerical simulations.

Sl. No	Name of Earthquake	Soil Type	Desig-nation	Magni-Tude	PGA (g)	Duration (s)
1	Kobe 1995/01/16	Soft Soil	FSR1-(EW)	M6.9	0.345	20
2	Kobe 1995/01/16		FSR2-(NS)	M6.9	0.251	20
3	Imperial Valley 1979/10/15		FSR3	M6.5	0.221	20
4	Northridge 1994/01/17	Alluvium Soil	FMR1	M6.7	0.364	20
5	Imperial Valley 1979/10/15		FMR2	M6.5	0.275	20
6	Chi-Chi Taiwan 1999/09/20		FMR3	M7.6	0.246	70
7	Loma Prieta 1989/10/18	Hard Soil/ Rock	FHR1	M6.9	0.41	20
8	Loma Prieta 1989/10/18		FHR2	M6.9	0.409	20
9	Kocaeli, Turkey 1999/08/17		FHR3	M7.4	0.244	20

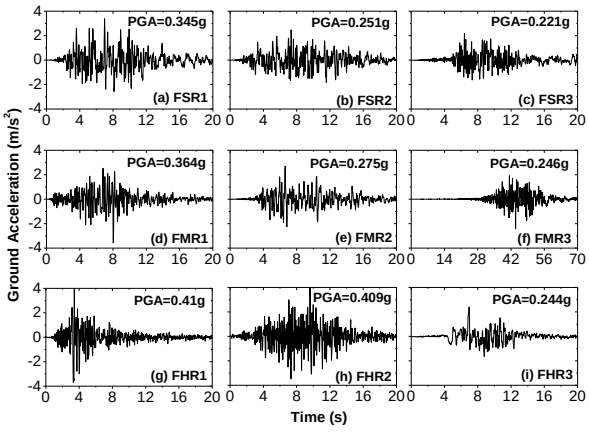

Figure 8: Ensemble of acceleration time-histories of ground motion records.

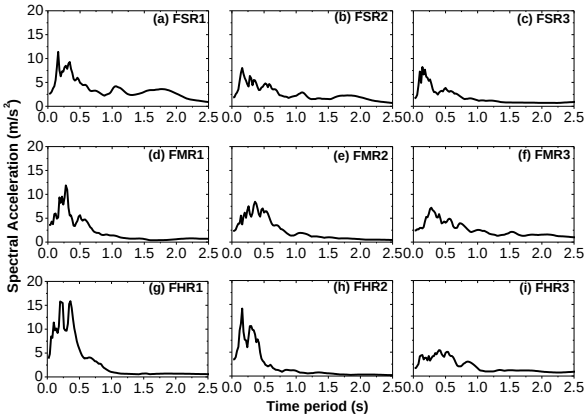

Figure 9: Ensemble of Acceleration spectra of ground motion records.

Acceleration Response Spectra

In this investigation, the variation of acceleration spectra of the SDOF structure with friction dampers for different pretension force has been evaluated for the nine earthquake ground motion records discussed above. Different stiffness ratios (SR= Kb/Ks), i.e. the ratio of stiffness of braced frame structure (Kb) to the stiffness of free frame structure (Ks), have been selected to study the influence of stiffness on the variation of Absolute acceleration response spectra of the structure with pretension force when subjected to the mentioned ground motions. The stiffness ratios selected in this study are 0.5, 1.0, 2.0, 4.0, 6.0, 8.0 and 10.0. The pretension forces considered in this study are in the range of 10 kN to 1010 kN with an interval of 100 kN. The variation of absolute acceleration response with reference to the pretension force for different time period (i.e. Absolute acceleration vs Pretension force vs Time period) has been presented for different stiffness ratios.

The variation of absolute acceleration response spectra with reference to pretension force subjected to FSR1 ground motion has been demonstrated in Figure 10. As evident from the results, with increase in stiffness ratio the peak absolute acceleration response increases. For lower stiffness ratio (i.e. for SR=0.5 and SR=1.0) the absolute acceleration response can not be controlled with increase in pretension force. However, with the increase in stiffness ratio, decreasing trend in the response is observed for pretension force range up to 400kN. At higher pretension force, for stiffness ratio 8.0 and 10.0, the structure behaves as braced frame with limited energy dissipation resulting in higher absolute acceleration response due to high stiffness.

Similar responses are observed in the example structure when subjected to FSR2 and FSR3 ground motions. Figure 11 indicate that the effectiveness of the damper increases with increase in pretension force from 100 kN to 400 kN at a higher stiffness ratio as the absolute acceleration response spectra tends to have a lower value in pretension force range of 100-300 kN, and the effectiveness dissipates with an increase of pretension force beyond 400 kN for the example structure when subjected to FSR2 ground motion. Similar response behaviour is observed for FSR3 ground motion in Figure 12.

From Figure 13, it is seen that the friction device is not effective at lower stiffness ratio, i.e. 0.5 and 1.0 when subjected to FMR1 ground motion, as with increase of pretension force beyond 300 kN no change in maximum response is observed with increase in pretension force. A downward trend is observed in the response to increase in the time period of the structure. As the stiffness ratio is increased beyond 2.0, the effective range of pretension force is increased, where the absolute acceleration response is low. The decreasing response pattern is also observed in a range of time period up to 0.4 secs. With the increase of the time period beyond 0.4 secs the absolute acceleration response increases abruptly up to 1.0 and then it decreases with an increase in the time period. Similar response behaviour is observed for FMR2 (Figure 14) and FMR3 (Figure 15) ground motions. For stiffness ratio of 8.0 and 10.0 and time periods up to 0.6 secs the absolute acceleration response is observed to be low for the example SDOF structure when subjected to FMR2 ground motion. For FMR3 ground motion damper acts effectively for the range of pretension force up to 300 kN and structural time period up to 0.5 secs for Stiffness ratios 8.0 and 10.0, where the absolute acceleration is low. In lower stiffness ratio of 0.5 and 1.0, the damper is found to be ineffective as no considerable change in response is observed to increase in pretension force.

The absolute acceleration spectra for the example SDOF structure when subjected to ground motions in hard soil (i.e. FHR1, FHR2 and FHR3) are presented in Figure 16, Figure 17 and Figure 18. For ground motion FHR1, the response is not found to be affected by the presence of the device for stiffness ratio 0.5 (as in Figure 16). The effectiveness is observed to be increased with the increase in bracing stiffness. The response is found to be reduced at a higher stiffness ratio of 8.0 and 10.0 for a fundamental time period up to 0.6 secs and for a range of pretension force of 100kN to 300kN. Similar response behaviour is observed for FHR2 and FHR3 ground motions. For FHR2 ground motion the response is observed (Figure 17) to be reduced considerably for lower stiffness ratios, i.e. 0.5, 1.0 and 2.0, with increase in the fundamental time period of the structure. However, in case of FHR3 (Figure 18) ground motions the reduced responses are observed for a fundamental time period up to 0.4 secs and for a range of pretension force up to 100 kN.

It is seen that the performance can be robust and relatively insensitive to ground motion characteristics. However, the performance depends on the pretension force as well as the stiffness ratio.

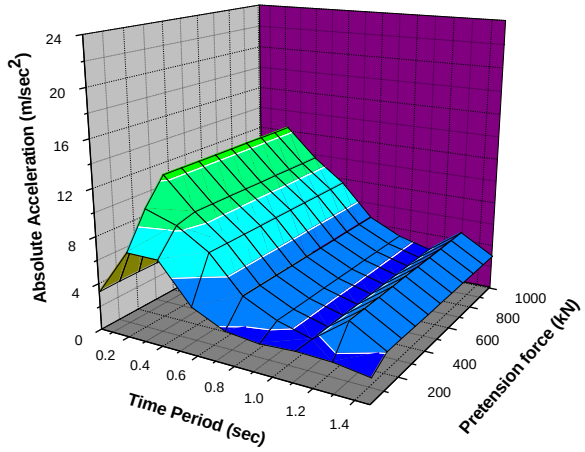

(Stiffness ratio= 0.5)

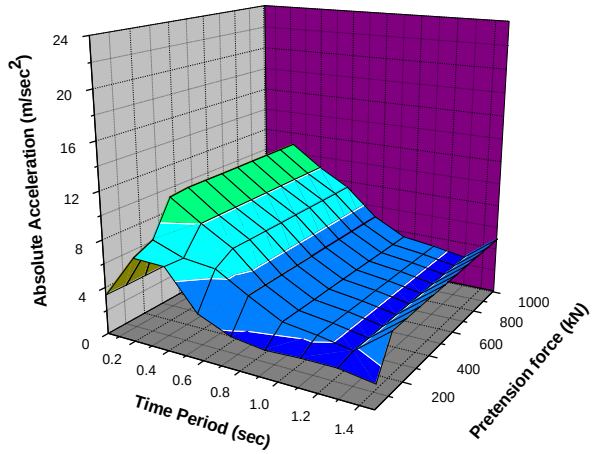

(Stiffness ratio= 1.0)

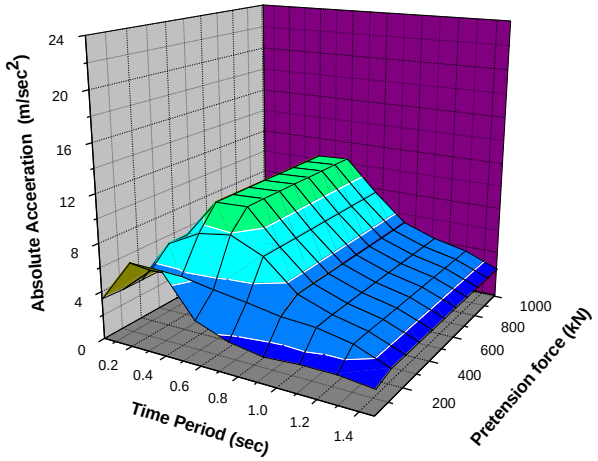

(Stiffness ratio= 2.0)

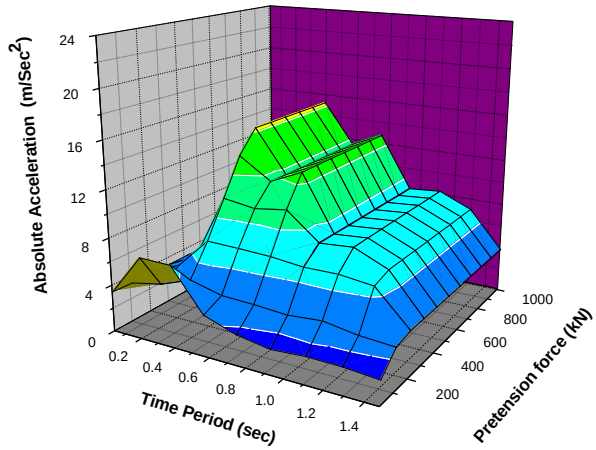

(Stiffness ratio= 4.0)

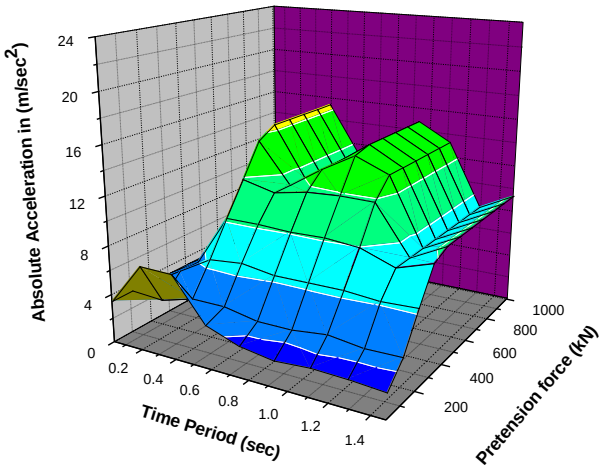

(Stiffness ratio= 8.0)

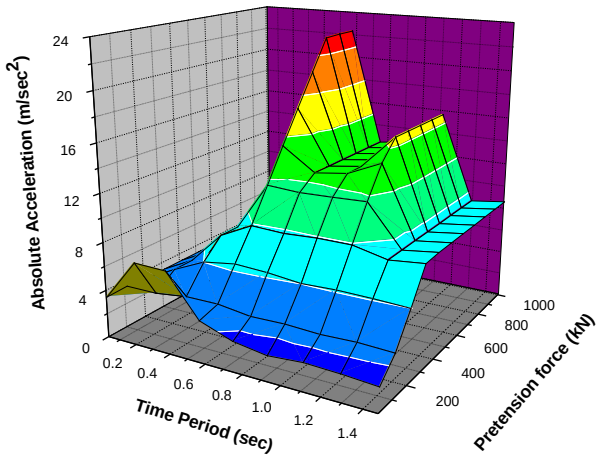

(Stiffness ratio= 10.0)

Figure 10. Absolute acceleration spectra at different pretension forces subjected to FSR1 ground motions.

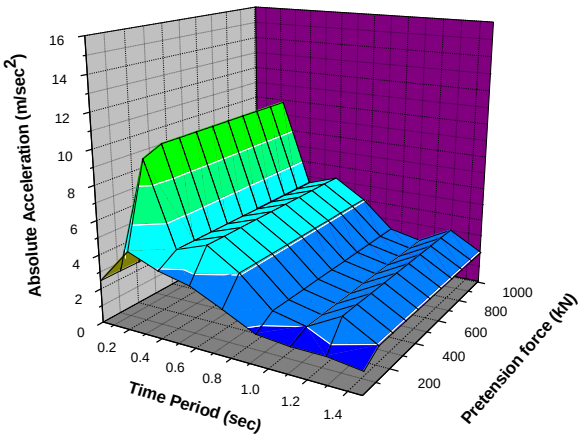

(Stiffness ratio= 0.5)

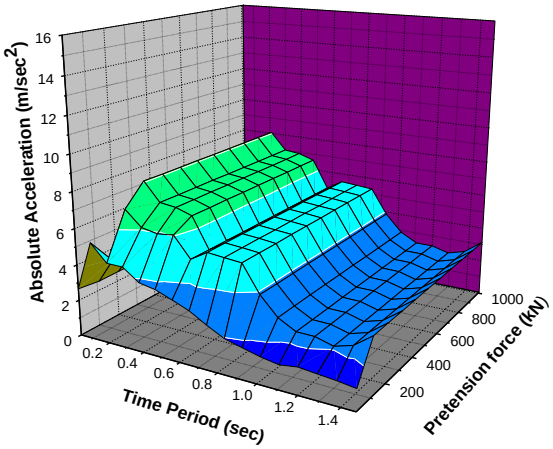

(Stiffness ratio= 1.0)

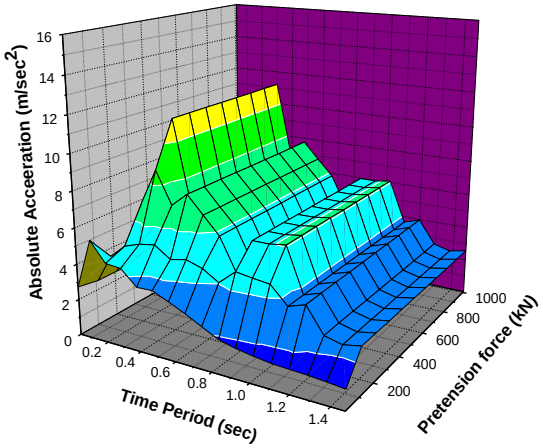

(Stiffness ratio= 2.0)

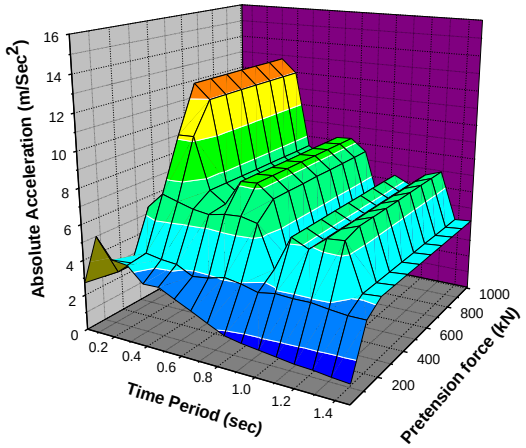

(Stiffness ratio= 4.0)

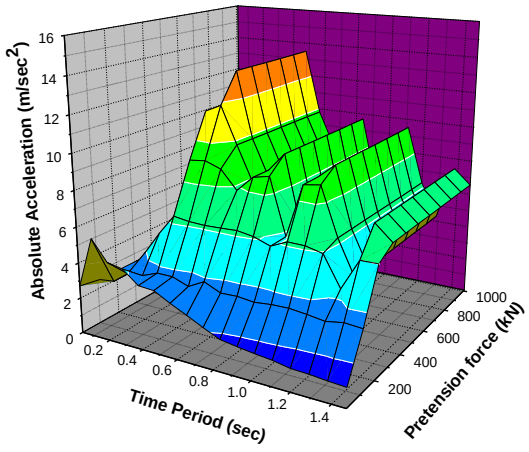

(Stiffness ratio= 8.0)

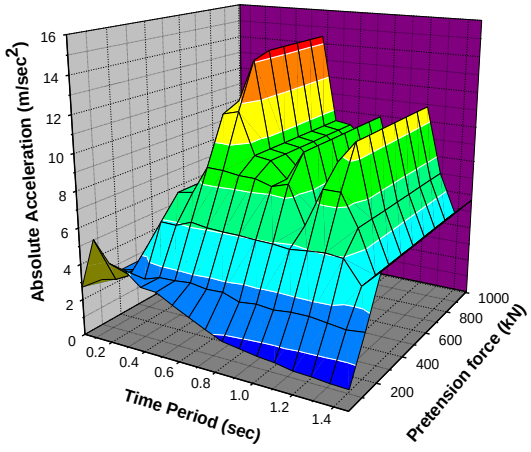

(Stiffness ratio= 10.0)

Figure 11. Absolute acceleration spectra at different pretension forces subjected to FSR2 ground motions.

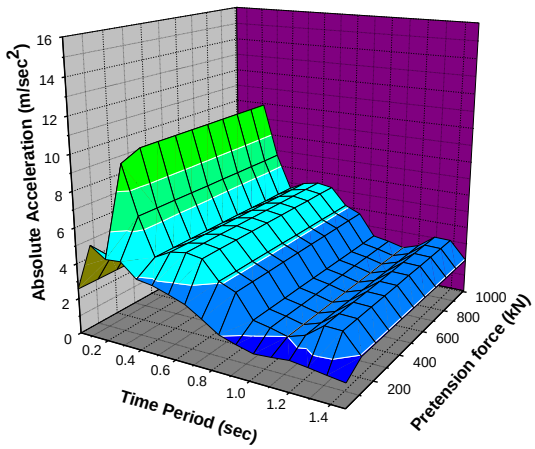

(Stiffness ratio= 0.5)

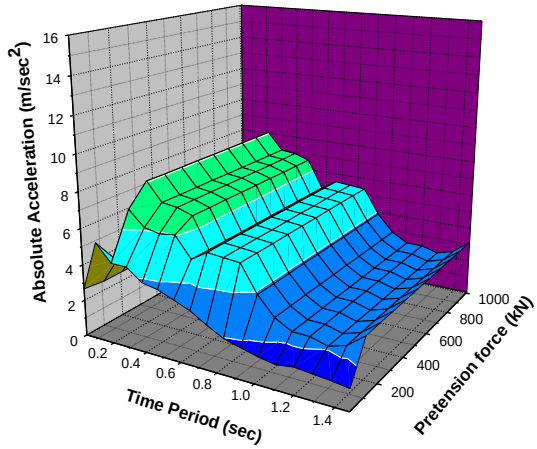

(Stiffness ratio= 1.0)

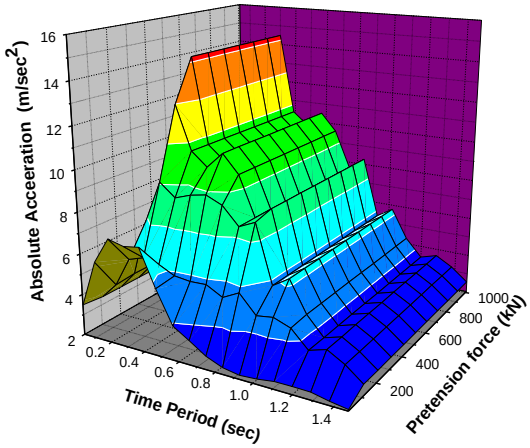

(Stiffness ratio= 2.0)

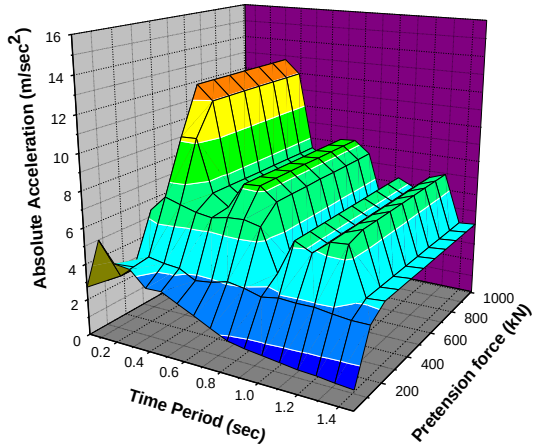

(Stiffness ratio= 4.0)

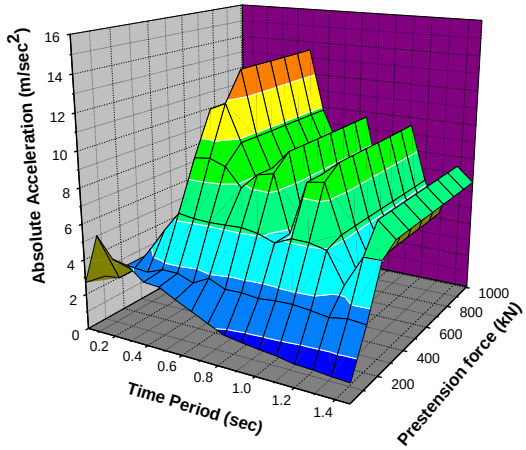

(Stiffness ratio= 8.0)

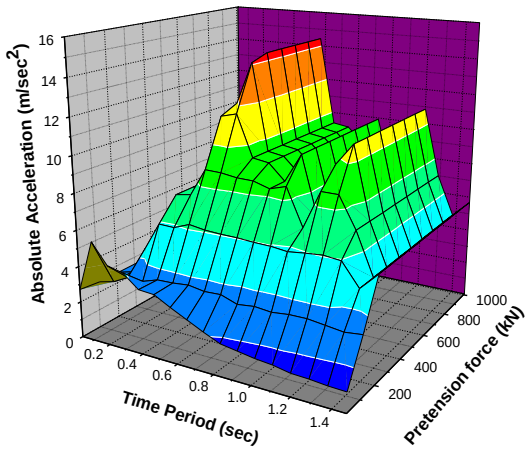

(Stiffness ratio= 10.0)

Figure 12. Absolute acceleration spectra at different pretension forces subjected to FSR3 ground motions.

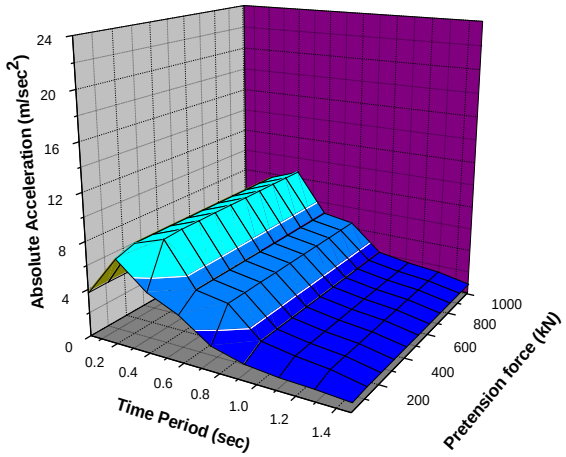

(Stiffness ratio= 0.5)

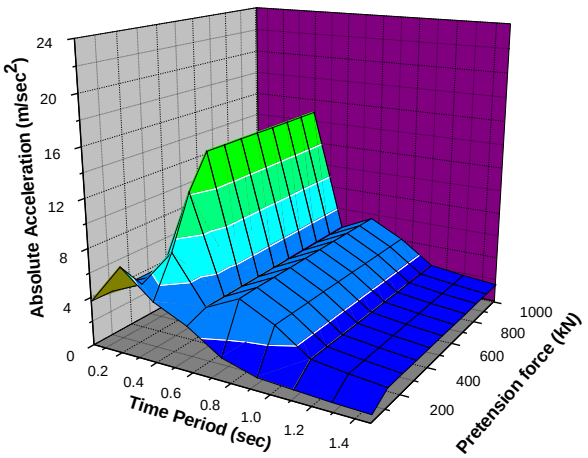

(Stiffness ratio= 1.0)

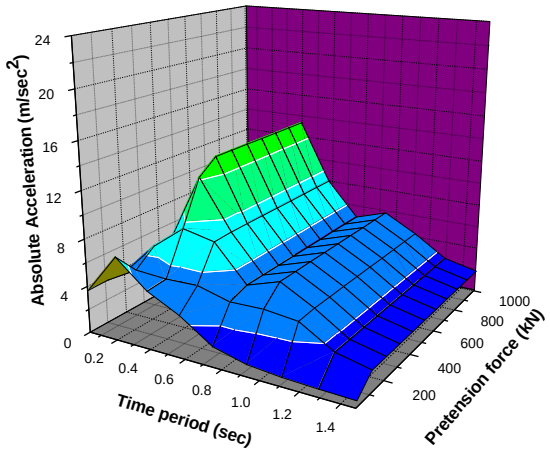

(Stiffness ratio= 2.0)

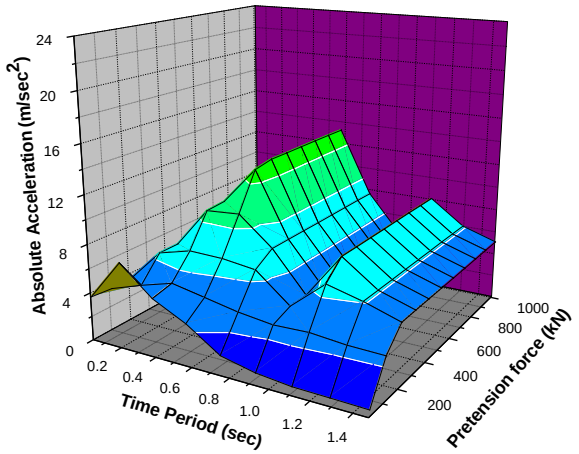

(Stiffness ratio= 4.0)

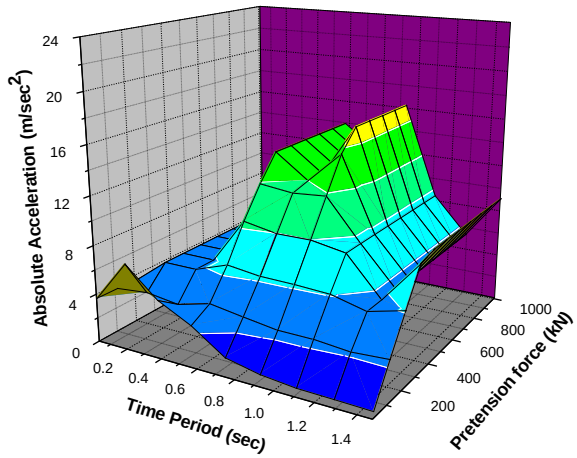

(Stiffness ratio= 8.0)

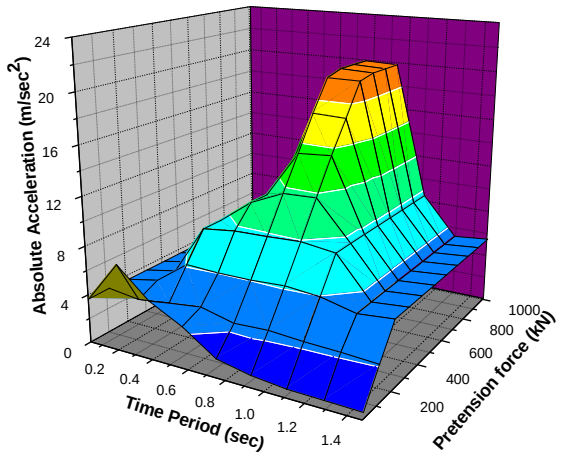

(Stiffness ratio= 10.0)

Figure 13. Absolute acceleration spectra at different pretension forces subjected to FMR1 ground motions.

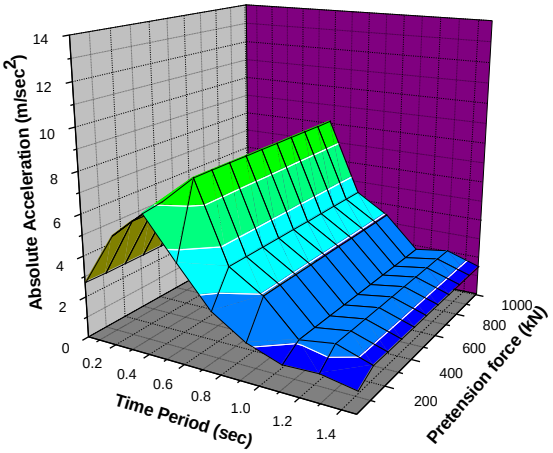

(Stiffness ratio= 0.5)

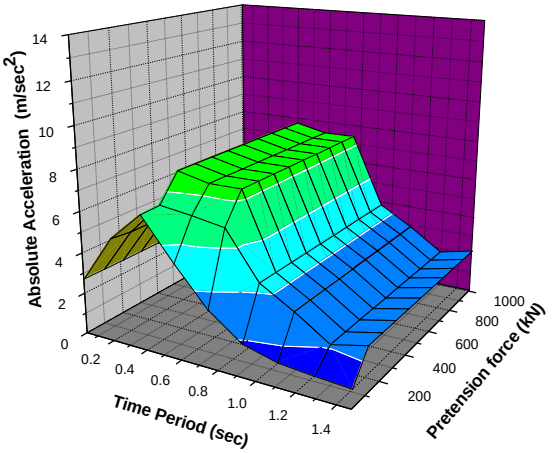

(Stiffness ratio= 1.0)

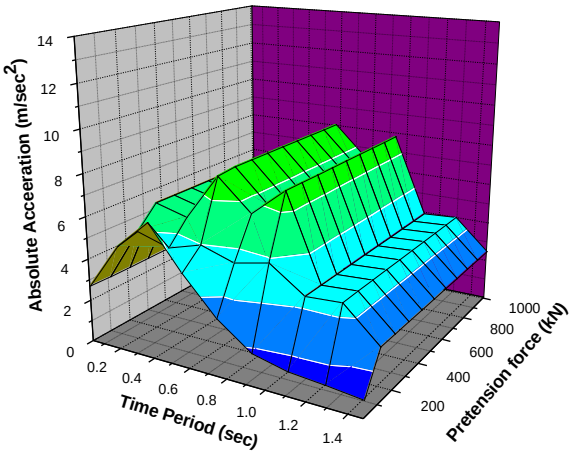

(Stiffness ratio= 2.0)

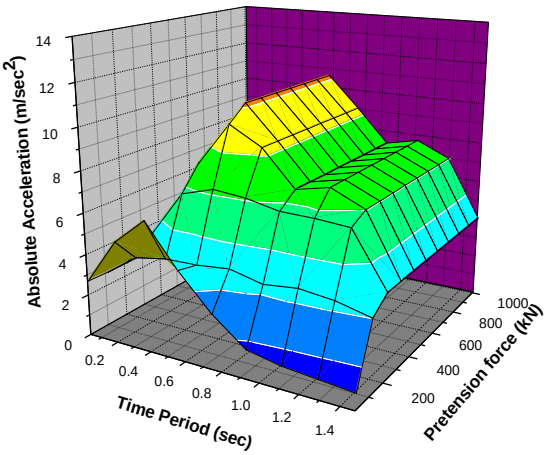

(Stiffness ratio= 4.0)

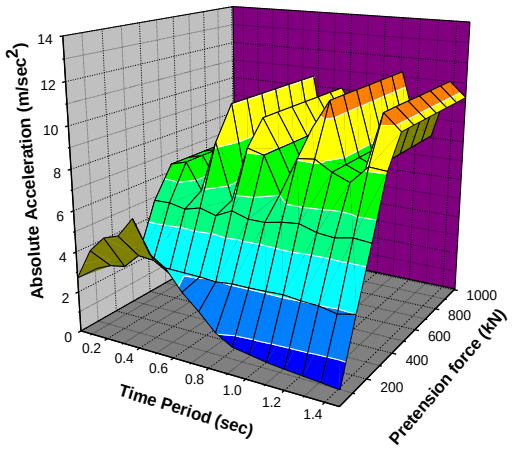

(Stiffness ratio= 8.0)

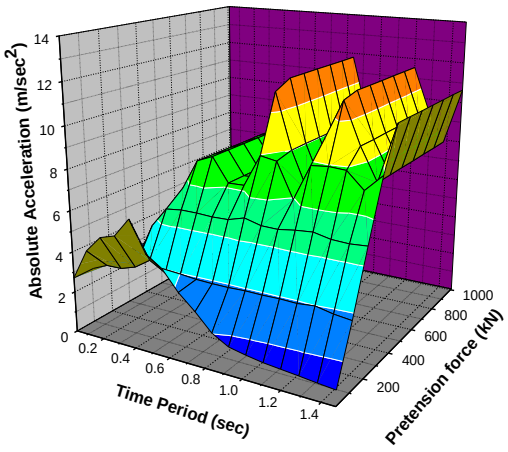

(Stiffness ratio= 10.0)

Figure 14. Absolute acceleration spectra at different pretension forces subjected to FMR2 ground motions.

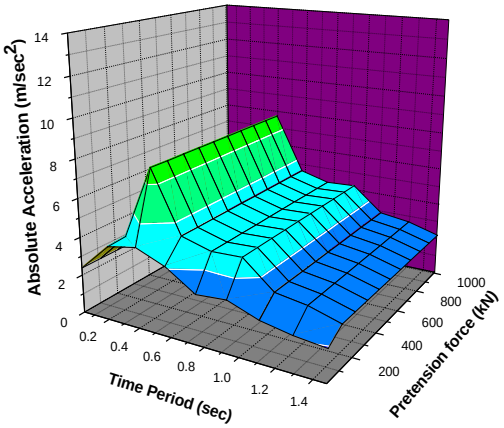

(Stiffness ratio= 0.5)

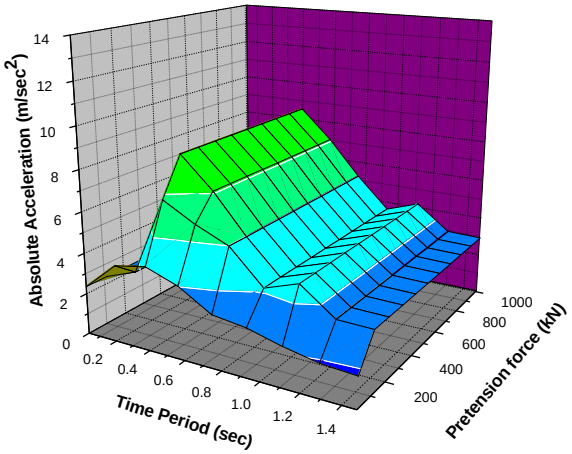

(Stiffness ratio= 1.0)

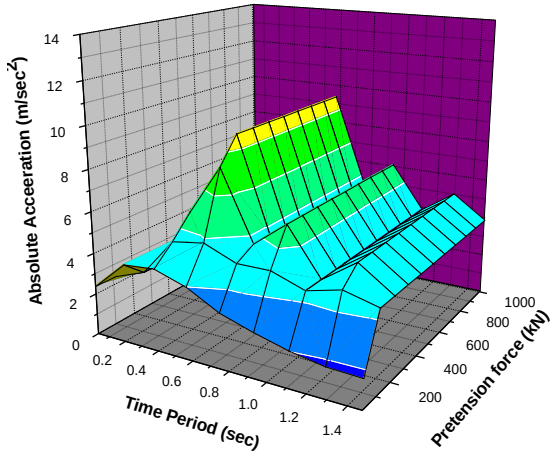

(Stiffness ratio= 2.0)

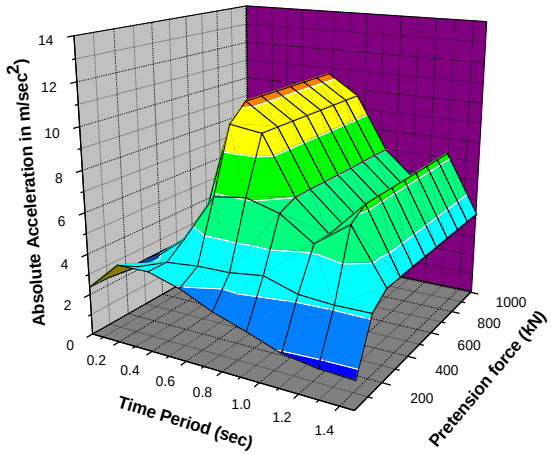

(Stiffness ratio= 4.0)

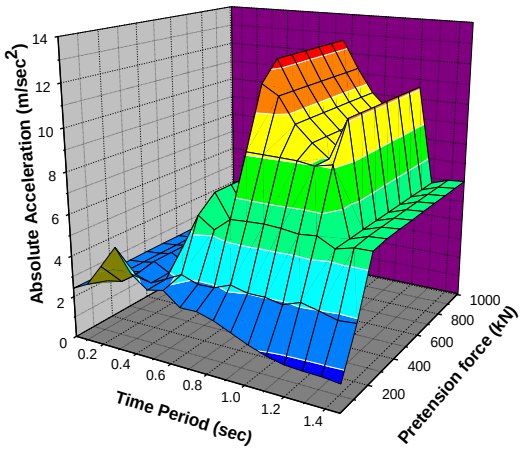

(Stiffness ratio= 8.0)

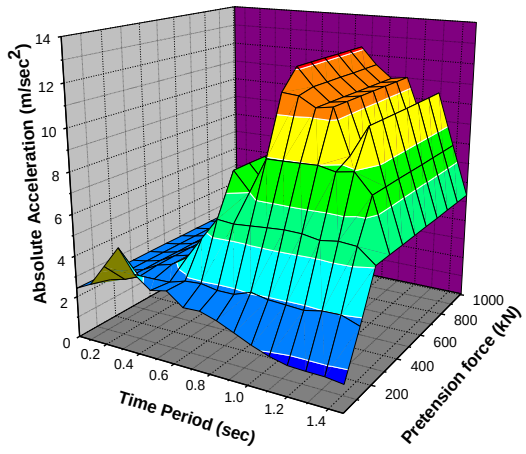

(Stiffness ratio= 10.0)

Figure 15. Absolute acceleration spectra at different pretension forces subjected to FMR3 ground motions.

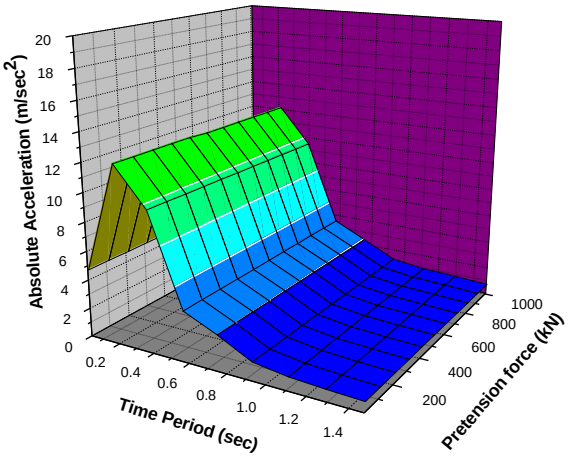

(Stiffness ratio= 0.5)

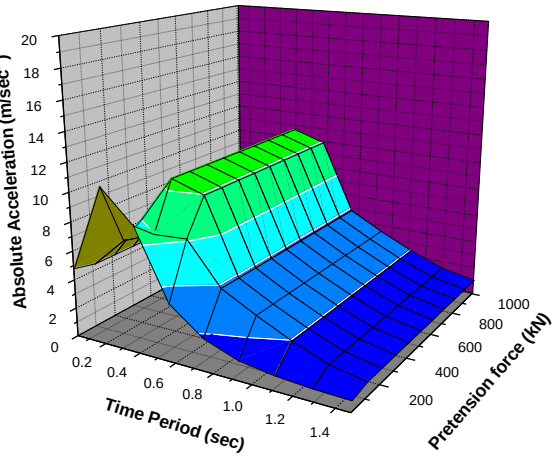

(Stiffness ratio= 1.0)

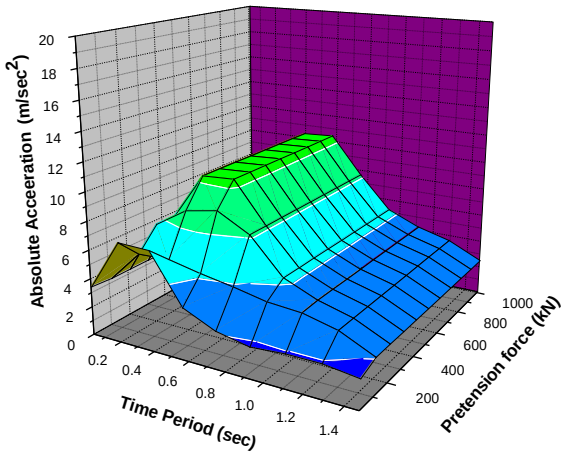

(Stiffness ratio= 2.0)

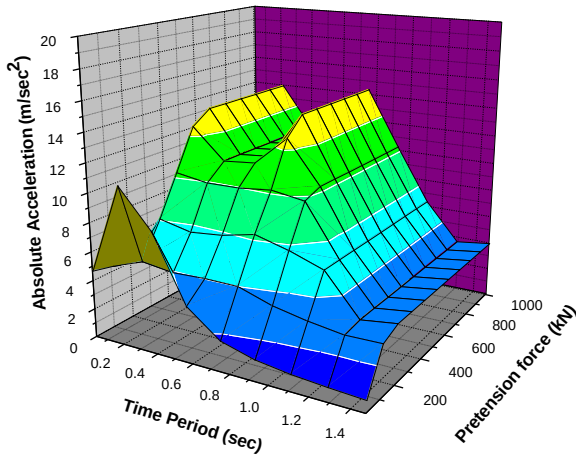

(Stiffness ratio= 4.0)

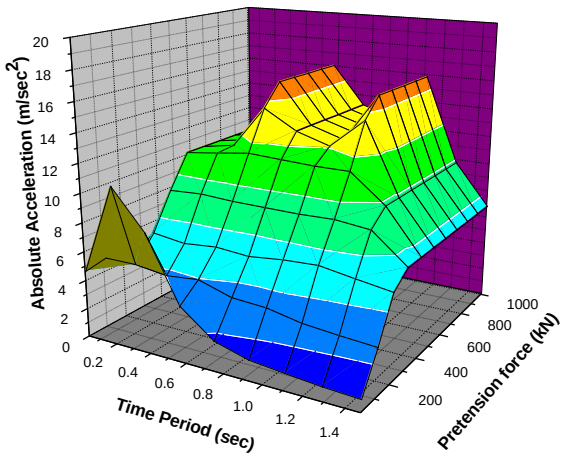

(Stiffness ratio= 8.0)

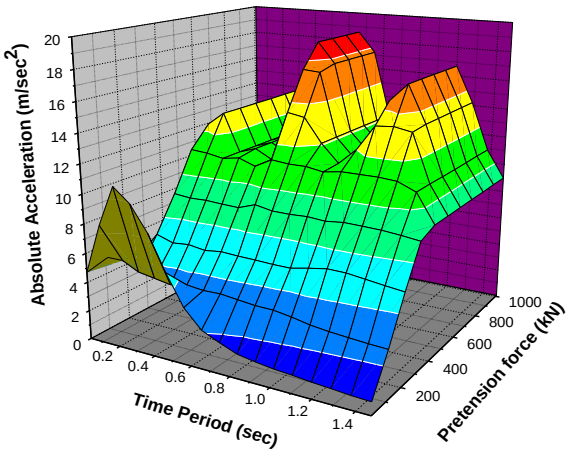

(Stiffness ratio= 10.0)

Figure 16. Absolute acceleration spectra at different pretension forces subjected to FHR1 ground motions.

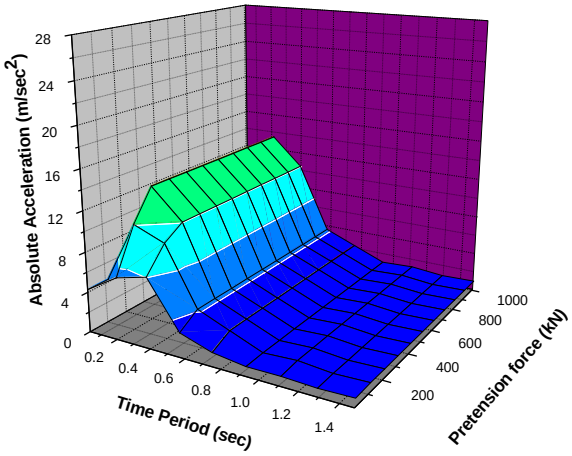

(Stiffness ratio= 0.5)

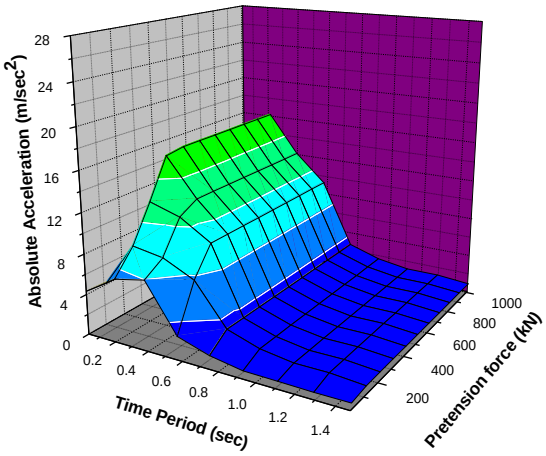

(Stiffness ratio= 1.0)

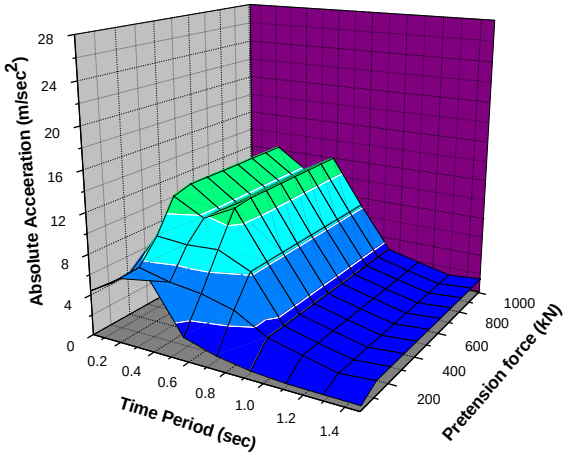

(Stiffness ratio= 2.0)

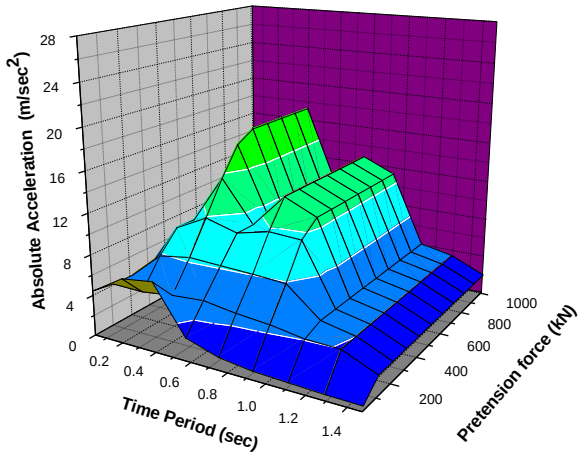

(Stiffness ratio= 4.0)

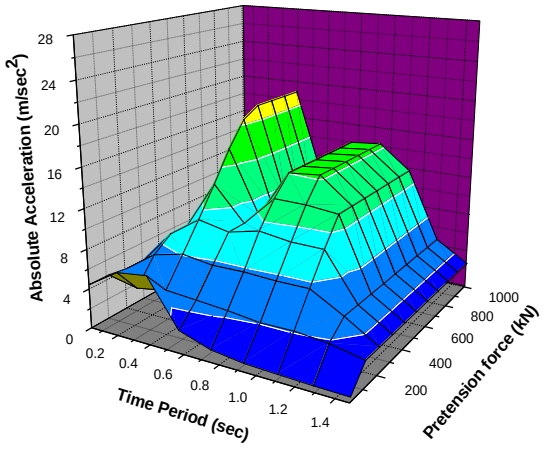

(Stiffness ratio= 8.0)

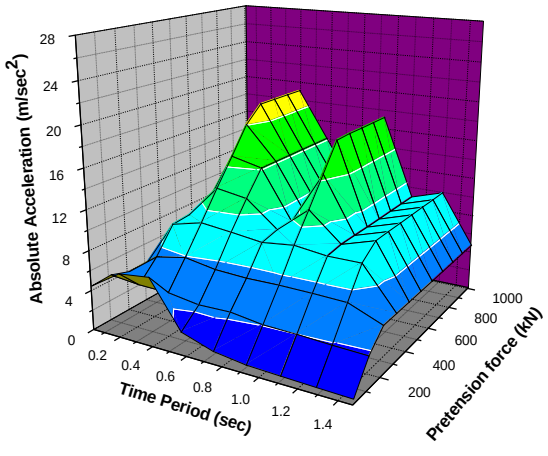

(Stiffness ratio= 10.0)

Figure 17. Absolute acceleration spectra at different pretension forces subjected to FHR2 ground motions.

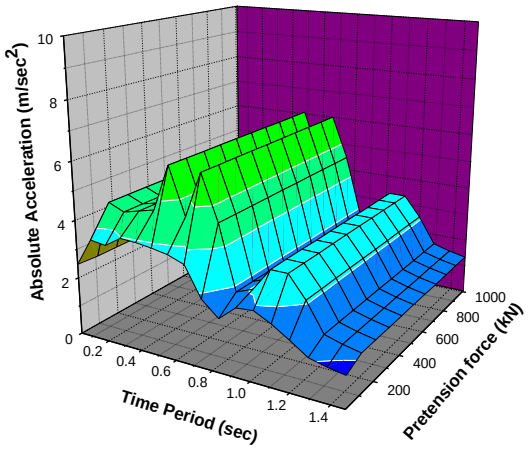

(Stiffness ratio= 0.5)

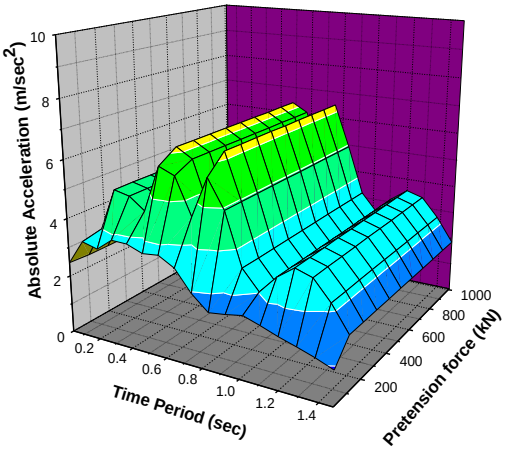

(Stiffness ratio= 1.0)

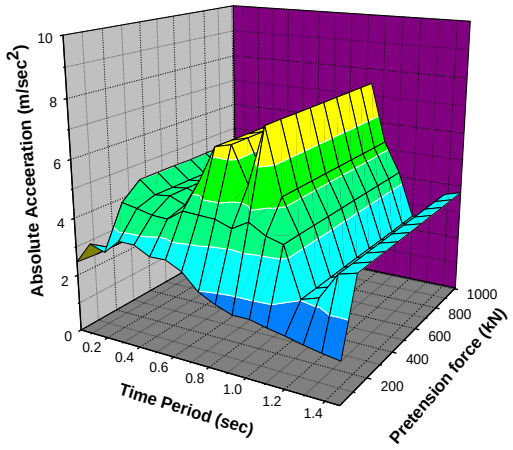

(Stiffness ratio= 2.0)

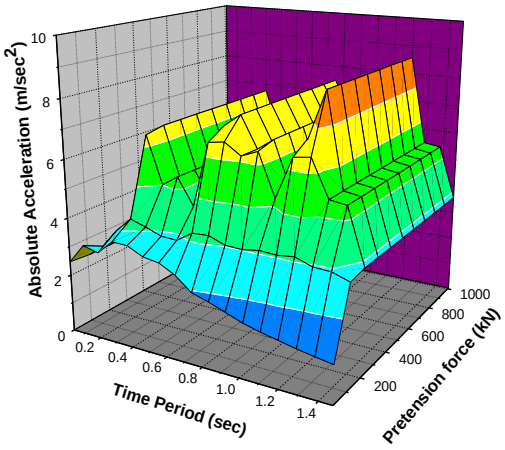

(Stiffness ratio= 4.0)

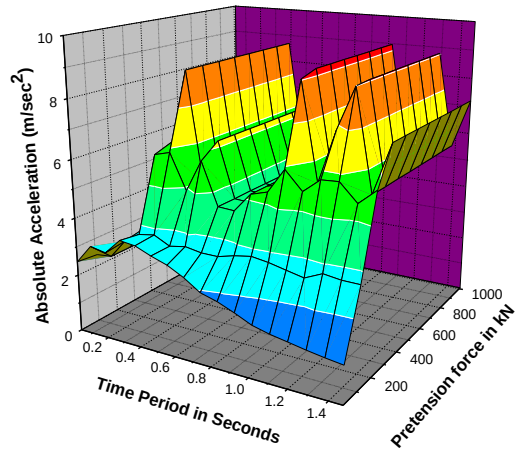

(Stiffness ratio= 8.0)

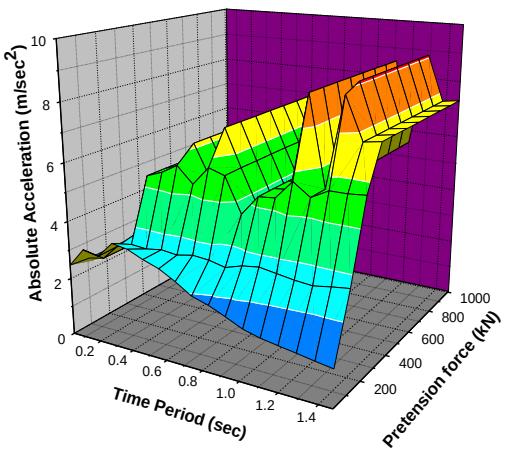

(Stiffness ratio= 10.0)

Figure 18. Absolute acceleration spectra at different pretension forces subjected to FHR3 ground motions.

DISCUSSIONS AND CONCLUSIONS

For the MDOF structure with friction devices the minimum difference in relative velocity or non-identification of exact time of phase transition results in a noticeably high fluctuation of relative velocity in the stick-slide model resulting in inaccuracy in the dynamic time history analysis. For avoiding these inaccuracies in the dynamic time history analysis, a numerical methodology has been demonstrated in the paper for determining the dynamic structural behaviour of the MDOF planar structures equipped with Slotted Bolted Connection (SBC) type friction slider mounted on Chevron brace. The proposed methodology has been compared with that of the published results to ascertain the validity and accuracy of the method. The excellent correlation between the published results and the results from the proposed methodology demonstrates the accuracy and adequacy of the present method in determination of dynamic behaviour of MDOF structure with friction damper. After successful validation, a SDOF structure with friction based energy dissipation system has been considered in evaluating the seismic performance of friction devices using the methodology. Acceleration spectrums for frame with friction devices have been evaluated for the range of pretension force from 10kN (Free frame) to 1010kN (Braced Frame) to determine the optimum pretension force and the fundamental time period at which the absolute acceleration is minimum. It has been found from the investigation that with increase in stiffness ratio beyond 4.0, the absolute acceleration response of the system is observed to be minimized for a range of pretension force of 100-250 kN for all ground motions for the considered frame. The acceleration spectrum response of the structure decreases with an increase in the fundamental time period of the system for both the free frame and braced frame. It is also observed that with increase in pretension force (i.e from free frame system to braced frame system) the response rises beyond the optimum absolute acceleration with an increase in the time period up to 0.4 sec and then decreases with an increase in the time period beyond 0.4 sec for the example system subjected to all ground motions. The study of response spectra of SDOF system with friction damper shows that the relative advantage of friction damper depends on stiffness ratio and pretension force. The extent of influence of these factors are accurately brought out in this paper due to the more precise modelling of friction in the equations of motion.

REFERENCES

1 Pall AS, Marsh C and Fazio P (1980). "Friction joints for seismic control of large panel structures". *Journal of Prestressed Concrete Institute*, **25**(6), 38-61.

2 Pall AS and Marsh C (1981). "Friction damped concrete shear walls". *Journal of American Concrete Institute*, **78**, 187-193.

3 Pall AS and Marsh C (1982). "Response of friction damped braced frames". *Journal of Structural Division*, ASCE, **108**(6), 1313-1323.

4 Pall AS (1983). "Friction devices for aseismic design of buildings". *Proceedings of the 4th Canadian Conference on Earthquake Engineering*, Vancouver, Canada, 475-484.

5 Filiatrault A and Cherry S (1987). "Performance evaluation of friction damped braced steel frames under simulated earthquake loads". *Earthquake Spectra*, **3**(1), 57-78.

6 Filiatrault A and Cherry S (1988). "Comparative performance of friction-damped systems and base isolation systems for earthquake retrofit and aseismic design". *Earthquake Engineering and Structural Dynamics*, **16**(3), 389-416.

7 Filiatrault A and Cherry S (1990). "Seismic design spectra for friction-damped structures". *Journal of Structural Engineering*, **116**(5), 1334-1355.

8 Filiatrault A and Cherry S (1990). "Seismic design spectra for friction-damped structures". *Journal of Structural Engineering*, **116**(5), 1334-1355.

9 Moreschi LM (2000). "*Seismic Design of Energy Dissipation Systems for Optimal Structural Performance*". Ph.D. Thesis, Virginia Polytechnic Institute and State University, Blacksburg, Virginia.

10 Asahina D, Bolander JE and Berton S (2004). "Design optimization of passive devices in multi-degree of freedom structures". *13th World Conference on Earthquake Engineering*, Vancouver, BC, Canada, Paper no. 1600.

11 FitzGerald TF, Anagnos T, Goodson M and Zsutty T (1989). "Slotted bolted connection in aseismic design for concentrically braced connections". *Earthquake Spectra*, **5**(2), 383-391.

12 Grigorian CE, Yang TS and Popov EP (1993). "Slotted bolted connection energy dissipators". *Earthquake Spectra*, **9**(3), 491-504.

13 Dimova S, Meskouris K and Kratzig WB (1995). "Numerical technique for dynamic analysis of structures with friction devices". *Earthquake Engineering and Structural Dynamics*, **24,**881-898.

14 Levy R, Marianchik E, Rutenberg A and Segal F (2001). "A simple approach to the seismic design of friction damped braced medium-rise frames". *Engineering Structures*, 23, 250-259.

15 Martinez-Rueda JK (2002). "On the evolution of energy dissipation devices for seismic design". *Earthquake Spectra*, **18**(2), 309-346.

16 Housner GW, Bergman LA, Caughey TK, Chassiakos AG, Claus RO,Masri SF, Skelton RE, Soong TT, Spencer BF and Yao JTP (1997). "Structural control: past, present, and future". *Journal of Engineering Mechanics*, **123**(9), 897-971.

17 Iwan WD and Gates NC (1979). "Estimating earthquake response of simple hysteretic structures". *Journal of Engineering Mechanics Division*, ASCE, **105**(3), 391-405.

18 Wen YK (1976). "Method for random vibration of hysteretic systems". *Journal of Engineering Mechanics Division*, ASCE, **102**(2), 249-263.

19 Mostaghel N and Tanbakuchi J (1983). "Response of sliding structures to harmonic support motion". *Earthquake Engineering and Structural Dynamics*, **11**, 729-748.

20 Pranesh M and Sinha R (2000). "VFPI: An isolation device for aseismic design". *Earthquake Engineering Structural Dynamics*, **29**, 603-627.

21 De La Cruz S, Lopez-Almansa F and Taylor C (2004). "Shaking table tests of steel frames equipped with friction dissipators and subjected to earthquake loads". *13th World Conference on Earthquake Engineering*, Vancouver, B. C., Canada, Paper no. 1525.

22 Dimova S, Meskouris K and Kratzig WB (1995). "Numerical technique for dynamic analysis of structures with friction devices". *Earthquake Engineering and Structural Dynamics*, **24**, 881-898.

23 Levy R, Marianchik E, Rutenberg A and Segal F (2001). "A simple approach to the seismic design of friction damped braced medium-rise frames". *Engineering Structures*, 23, 250-259.

24 Lu LY, Chung LL, Wu LY and Lin GL (2006). "Dynamic analysis of structures with friction devices using discrete-

time state-space formulation". *Computers and Structure*, 84, 1049–1071

25 Pall AS and Marsh C (1980). "Optimum seismic resistance of large panel structures". Proc. *7th World Conference on Earthquake Engineering*, Istanbul, Vol. 4, 177-184

26 Wakabayashi M , Fudjiwara T, Nakamura T and Basotov T (1982). "Experimental and analytical responses of isolated structures". *Proc. 7th European Conference on Earthquake Engineering*, Athens, Vol. 4, 463-470

27 Filiatrault A, Cherry S (1986). "Tests of the behavior of friction dampers in braced steel frames". *Proc. 8th European Conference on Earthquake Engineering*, Lisbon, Vol. 5, 85/41-481.

28 Grigorian CE and Popov E (1993). "Slotted bolted connections for energy dissipation". *Proc. ATC-17-I seminar on base isolation and passive energy dissipation*, San Francisco, Vol. 3, 545-556

29 Aiken ID and Kelly JM (1990). "*Earthquake simulator testing and analytical studies of two energy absorbing systems for multistory structures*". Report No. UCB/EERC-90/03, Earthquake Engineering Research Center, University of California, Berkeley, CA

30 Juhasova E and Oprcal M (1986). "Some problems of efficiency of seismic sliding isolation systems". *Proc. 8th European conference on earthquake engineering*, Lisbon, Vol. 5, 84/17-23.

31 Mostaghel N and Tanbakuchi J (1983). "Response of sliding structures to earthquake support motion". *Earthquake Engineering and Structural Dynamics*, 11, 729-748.

32 Mostaghel N and Khodaverdian M (1987). "Dynamics of resilient friction base isolator (R-FBI)". *Earthquake Engineering and Structural Dynamics*, 15,379-390.

33 Su L, Ahmadi G and Tadjbakhsh I (1989). "A comparative study of performances of various base isolation systems. Part I: Shear beam structures". *Earthquake Engineering and Structural Dynamics*, 18, 11-32.

34 Feldstein A and Goodman R (1973). "Numerical solution of ordinary and retarded differential equations with discontinuous derivatives". *Numerische Mathematik*, 21, 1-13.

35 Bhatti MA and Pister KS (1981). "Transient Response Analysis of Structural Systems with Nonlinear Behavior". *Computers and Structures*, 13, 181-188.

36 Swain SS and Patro SK (2015). "Seismic Protection of Soft Storey Buildings using Energy Dissipation Device". *Advances in Structural Engineering: Dynamics, Vol-2*, 1311-1338

37 Chopra AK (2001). "*Dynamics of Structures: Theory and Applications to Earthquake Engineering*". 2nd edition, Prentice Hall, New Delhi, 844pp.